BIOCHEMICAL AND FUNCTIONAL CHARACTERIZATION OF PROTEINS ENCODED BY SARS-CoV SUBGENOMIC mRNA 8

TRA MY LE

NATIONAL UNIVERSITY OF SINGAPORE

2006

BIOCHEMICAL AND FUNCTIONAL CHARACTERIZATION OF PROTEINS ENCODED BY SARS-CoV SUBGENOMIC mRNA 8

TRA MY LE

A THESIS SUBMITTED

FOR THE DEGREE OF MASTER OF SCIENCE

DEPARTMENT OF BIOLOGICAL SCIENCES

NATIONAL UNIVERSITY OF SINGAPORE

2006

ACKNOWLEDGEMENT

I would like to express my heart-felt appreciation and gratitude to my supervisors, Associate Professor Liu Ding Xiang for his mentorship, guidance, motivation and understanding. His influence indeed plays an important role in nurturing and inspiring me to pursue science as a career.

Also, my best regards to Dr Fang and Dr Yamada for their insightful suggestions and views on my project.

Special thanks to Dr Nasir and Huihui for taking time off to read and amend my draft, else it would have been gibberish everywhere.

Sincerely thanks to friends for their assistant and encouragement, especially Felicia, Xiaoxing, Yinchern and Benson for their valuable help and friendship throughout the years.

To everyone in LDX lab for their companionship and support, thanks to Dr Xu Linghui, Chen Guang, Xiaohan, Ronghua, Siti and Boon Hunt.

I would like to express my appreciation to Department of Biological Sciences (NUS) for their support and NUS for the research scholarship.

Finally, I would like thank my loving family and room mates for their support and understanding throughout these years especially when I'm writing up this thesis. I love you all!!!

CONTENTS

LIST OF PUBLICATION

RUNNING TITLE

Subgenomic mRNA 8 of Severe Acute Respiratory Syndrome-Associated coronavirus (SARS-CoV) Encodes a Novel Ubiquitin-binding Protein

Tra My Le, and D. X. Liu.

ABSTRACT

The most striking difference in the subgenomic mRNA8 of SARS-CoV isolated from human and some animal species is the deletion of 29 nucleotides, resulting in splitting of a single ORF (ORF 8) into two ORFs (ORF 8a and 8b). ORF 8a and 8b are predicted to encode two small proteins, 8a and 8b, and ORF 8 a single protein 8ab (a fused form of 8a and 8b proteins). To understand the functions of these proteins, we cloned cDNA fragments covering these ORF into expression plasmids, and expressed these constructs in in vitro and in vivo systems. It was shown that expression of a construct containing ORF 8a and 8b generated only a single protein 8a; no detection of the 8b expression was obtained. Expression of a construct containing ORF 8 generated the 8ab fusion protein. Subcellular localization studies of HeLa cells expressing protein 8a, 8b and 8ab showed that 8a and 8ab are localized to the cytoplasm, and 8b in the ER. Site-directed mutagenesis and enzymatic treatment revealed that 8b and 8ab were modified by N-linked glycoprotein, and by ubiquitination. More interestingly, the two proteins could form complex with ubiquitin and interferon regulatory factor 3, suggesting the potential involvement of these protein in the pathogenesis of SARS-CoV.

LIST OF ABBREVIATIONS

aa	Amino acid
DNA	Deoxyribonucleic acid
ER	Endoplasmic reticulum
GST	Gluthionine S-transferase
IB	Immunoblotting
kDa	Kilodalton
Nsp	Non-structural protein
ORF	Open reading frame
PCR	Polymerase chain reaction
RNA	Ribonucleic acid
RPM	Round per minute
RRL	Rabbit reticulocyte lysates
SARS	Severe acute respiratory syndrome
SARS-CoV	Severe acute respiratory syndrome associated coronavirus
SDS-PAGE	Sodium dodecyl sulfate-polyacrylamide gel electrophoresis
TRS	Transciption-regulatory sequence
UTR	Untranslated region
WG	Wheat germ extracts
WHO	World Health Organization

LIST OF FIGURES

LIST OF TABLES

SUMMARY

Coronavirus is a common etiologic agent of respiratory and enteric diseases in human and animals. Recently, a severe acute respiratory syndrome outbreak (SARS) in human was found to be caused by a new coronavirus, named SARS-CoV. It was suspected to have a natural reservoir host in animals. In fact, SARS-like coronaviruses were found in civets, ragoons and bats. Without vaccine and effecious treatment, SARS-CoV has impacted heavily on economical and social activities. Therefore, it is important to understand what attribute to the jumping of SARS-CoV from animals to human in order to monitor the possible reemergence of the outbreak.

Of isolated SARS-CoV and SARS-like coronaviruses, the most striking difference was found in the subgenomic mRNA 8. In human isolates collected at the late stage of the outbreak, subgenomic mRNA 8 of SARS-CoV was found with 29 nucleotide deletion. It resulted in the splitting of a single ORF (ORF8) into two ORFs (ORF 8a and 8b). ORF 8a and 8b are predicted to encode two small proteins, 8a and 8b, and ORF 8 a single protein 8ab (a fused form of 8a and 8b proteins). This deletion is hypothesized as the adaptation of SARS-CoV from animals to human. To understand the functions of these proteins, cDNA fragments covering these ORF were cloned into expression plasmids, and expressed in *in vitro* and *in vivo* systems. It was shown that expression of a construct containing ORF 8a and 8b generated only a single protein 8a; no detection of the 8b expression was obtained. Expression of a construct containing ORF 8 generated the 8ab fusion protein. Subcellular localization studies of HeLa cells expressing protein 8a, 8b and 8ab showed that 8a and 8ab are localized to the cytoplasm, and 8b in the ER. Site-directed mutagenesis and enzymatic treatment revealed that 8b and 8ab were

modified by N-linked glycoprotein and ubiquitination. More interestingly, the two proteins could form complex with ubiquitin and interferon regulatory factor 3, suggesting the potential involvement of these proteins in the pathogenesis of SARS-CoV.

CHAPTER 1. LITERATURE REVIEW

1.1. Classification of Coronaviruses

Coronaviruses belong to one genus *Coronavirus* in the family *Coronaviridae* and are large, enveloped, positive and single stranded RNA viruses. They occupy the largest genome of all RNA viruses with a unique transcription mechanism (Lai and Cavanagh 1997; Lai and Holmes 2001).

Coronaviruses are known as a diverse group with a wide range of hosts from avian to mammalian species (Murray *et.al.*1992; Lai and Holmes 2001). On the basis of serological analysis and antibody cross-reactivity tests, coronaviruses were classified into three main groups (Table 1.1).

1.2. Severe Acute Respiratory Syndrome (SARS)

SARS is the first new infectious disease of this century and it spread globally within a few months (WHO report 2003).

In late 2002, atypical pneumonia appeared in the province of Guangdong, in South China. It was initially reported with several hundred cases with unknown etiology. By March 2003, the disease had spread accidentally to Hong Kong, then to Singapore, and subsequently to Vietnam, Canada and United States by air travelers. The disease soon became a worldwide epidemic. By late April 2003, up to 25 countries were affected by the epidemic. With the efforts of governments, doctors and scientists, the epidemic was finally declined after 114 days. The total number of SARS patients worldwide was 8098 with 774 deaths. Without vaccine and efficacious treatment, the disease affected a total of 29 countries with serious disruption to normal life. It almost paralyzed global

Table 1.1. Serotypes, natural hosts and infection type of Coronavirus (Lai and Holmes 2001)

Antigenic group	Species	Host	Diseases			
			Respiratory infection	Enteric infection	Hepatitis	Neurologic infection
I	HCoV-229E	Human	X			
	TGEV, PRCoV	Pig	X	X		
	CCoV	Dog		X		
	FECoV	Cat		X	X	X
	FIPV	Cat	X	X		
	RbCoV	Rabbit	X	X		
II	HCoV-OC43	Human	X			
	MHV	Mouse	X	X	X	X
	SDAV	Rat				
	HEV	Pig	X	X		X
	BCoV	Cow	X	X		
III	IBV	Chicken	X		X	
	TCoV	Turkey	X	X		

HCoV-229E, human respiratory coronavirus; TGEV, Porcine transmissible gastroenteritis virus; PRCoV, porcine respiratory coronavirus; CCoV, canine coronavirus; FECoV, heline enteric coronavirus; FIPV, feline infectious peritonitis virus; RbCoV, rabbit coronavirus; HCoV-OC43, human respiratory coronavirus; MHV, murine hepatitis virus; SDAV, sialodacryoadenitis virus; HEV, porcine hemagglutinating encephalomyelitis virus; BCoV, bovine coronavirus; IBV, avian infectious bronchitis virus; TCoV, turkey coronavirus.

economy with profound impact on tourism, education and employment (WHO report, 2003).

SARS is characterized with flu-like symptoms manifested with high fever exceeding 38°C, myalgia, dry nonproductive dyspnea, lymphopaenia, infiltrate on chest radiography and finally atypical pneumonia (Peiris *et.al.*2003 a and b). In March 2003, the etiologic agent of SARS was found to be a new coronavirus (SARS-CoV) (Drosten *et.al.,* 2003; Fouchier *et.al.,* 2003; Ksiazek *et.al.,* 2003; Ksiazek *et.al.,* 2003 Peiris *et.al.,* 2003 b).

SARS is spread via droplets. However, the efficiency of infection is low with an infectivity index of about 3 (Lipsitch *et.al.,* 2003). In some instances, a few patients were considered as super-spreaders by transmitting SARS-CoV to a large number of individuals (Riley *et.al.,* 2003). Till now, there is no explanation for this phenomenon. The mortality rate of SARS is approximately 10%, but it also depends on the age group. The mortality rate is found low in children but was high in the elderly with up to 50% mortality rate (Stadler *et al*., 2003; Hon *et.al.,* 2003).

1.3. Virion morphology of SARS-CoV

Like most coronaviruses, SARS-CoV appears, under electron microscopy, with a corona-like morphology (Fig. 1.1) (Stadler *et al*., 2003). The virus was observed with pleomorphic spherical particles of approximately 100nm in diameter (Marra *et.al.,* 2003; Rota *et.al.,* 2003). The viral envelope is prominently fringed and evenly dispersed with 20 nm-long projectors; it is composed of a lipid bilayer, associated with M and E

proteins, and is also incorporated with S proteins (Rota *et.al.* 2003). The positive, single stranded RNA genome was integrated with the N protein within the envelope.

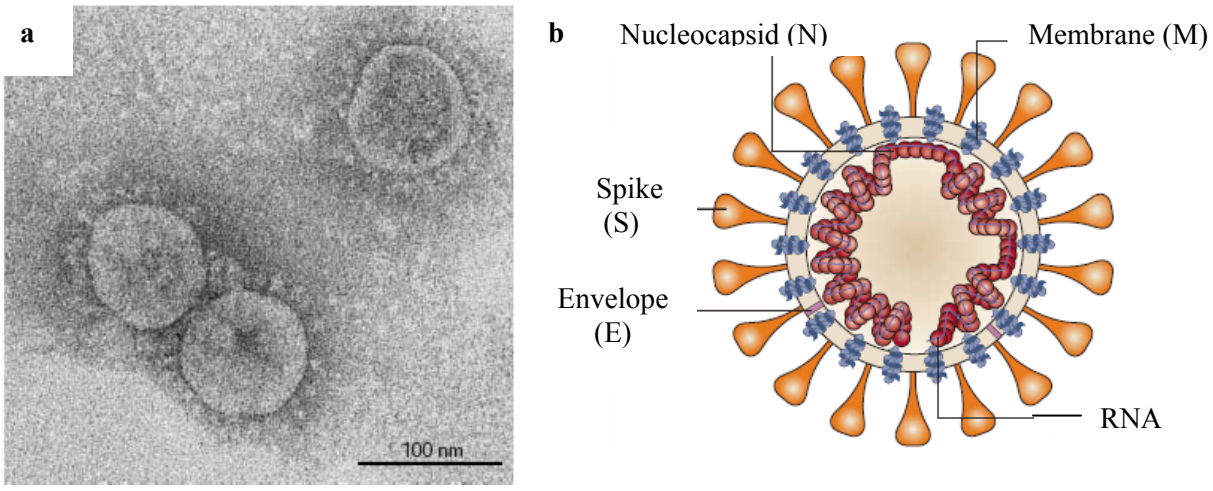

Figure 1.1. a. Electron micrograph of SARS-CoV. b. Schematic diagram of SARS-CoV Spike proteins (S: orange projectors) are radiated evenly on the lipid bilayer envelope. Together with S protein, membrane (M: blue) and envelope (E: pink) protein are associated with the lipid bilayer envelope. Nucleocapsid protein (N) integrated with viral RNA genome inside the viral envelope (Stadler *et al*., 2003).

1.4. Classification of SARS-CoV

Classification of SARS-CoV was initially determined based on the identity of the most conserved proteins between coronavirus strains such as RdRp, helicase, 3C-like protease and structural proteins. Using unrooted phylogenetic analysis, Marra and Rota 2003 simultaneously proposed that SARS-CoV represents a new group of coronavirus when they compared the sequence of the replicase proteins and the structural proteins of SARS-CoV to the other coronaviruses (Fig.1.2a). On the other hand, Snijer *et.al.,* 2003 used the rooted phylogenetic method and used the most conserved region encoded by ORF 1b as a criteria for comparison; they concluded that SARS-CoV is just an early split off from group 2 (Fig.1.2b). There is increasing evidence conceding SARS-CoV as a species of group 2 coronavirus. In fact, 80 percent of the whole SARS-CoV genome

sequence is closely related to group 2 coronavirus genome sequences (Magiorkinis *et.al.*, 2004). However, SARS-CoV does not encode the hemaglutinin esterease, one of the conserved proteins in group 2 coronaviruses (Stadler *et.al.*2003).

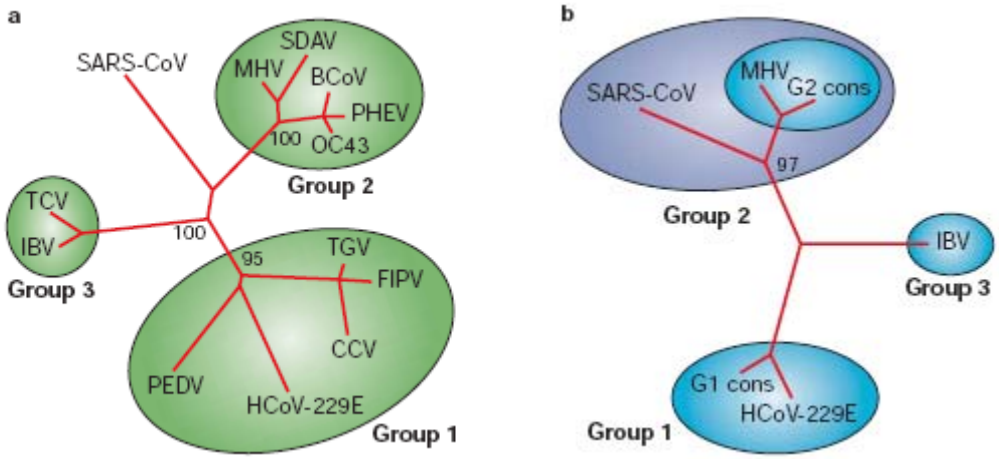

Figure 1.2. Phylogenetic analysis of Coronaviruses

a. unrooted phylogentic tree (Marra. *et. al.*, 2003) and b. rooted phylogenetic tree (Snijder *et. al.*, 2003)

1.5. Genome organization of SARS-CoV

SARS-CoV contains a large RNA genome of 29,727 nucleotides excluding its poly (A) tail (Rota *et.al.*, 2003; Marra *et.al.*, 2003). The genomic RNA begins with a leader sequence (nucleotides 1 to 72) followed by 192 nucleotides of untranslated region (UTR). Downstream of the 5' UTR is two overlapping open reading frames (ORFs) 1a and 1b that occupy two-thirds of the genome and encode the two polyproteins 1a and 1ab (Marra *et.al.*, 2003; Stadler *et.al.*, 2003). The remaining part of the genome is covered by ORFs coding for other SARS-CoV proteins. The SARS-CoV genome contains with 14 ORFs encoding structural proteins (S, E, M and N proteins) and accessory proteins (Marra *et.al.*, 2003). Of these ORFs, ORFs 3a, 3b, 6, 7a, 7b, 8a, 8b and 9b of SARS-CoV

genome do not show any homology with other coronaviruses (Marra *et.al.,* 2003; Rota *et.al.,* 2003; Ziebuhr 2004). The SARS-CoV genome ends with a 340 nucleotide UTR and a poly (A) tail (Ziebuhr, 2004).

In SARS-CoV genome and at the upstream region of most ORFs, there is a typical sequence (5' ACGAAAC 3') that is considered as a transcription-regulatory sequence (TRS) (Marra *et.al.,* 2003; Thiel *et.al.,* 2003). The TRS of SARS-CoV was determined by aligning manually the upstream region of potential initiating methionine codons (Sawicki *et.al.,* 1998). Together with the leader sequence, the 5' and 3' UTR, TRS directs the transcription and translation of coronavirus (Lai and Cavanagh, 1997; Stadler *et.al.,* 2003). The schematic representation of SARS-CoV genome is summarized in Fig.1.3.

1.6. Structure of subgenomic mRNAs and negative strand RNA of SARS-CoV

One of the most distinct features of coronaviruses is the synthesis of different species of subgenomic mRNA with 3' co-terminal, nested-set structure. All the subgenomic mRNAs start with the same sequence at the 3' terminus and extend to various distances toward the 5' end. Most of the genomic mRNAs of coronaviruses are structurally polycistronic but only the 5' most ORF of each subgenomic can be translated (Lai and Cavanagh, 1997). However, in some cases, one mRNA can encode several proteins. For example, sugenomic mRNA3 of Infectious Bronchitis Virus (IBV) encodes 3 proteins, 3a, 3b and E (Liu *et.al.,* 1992).

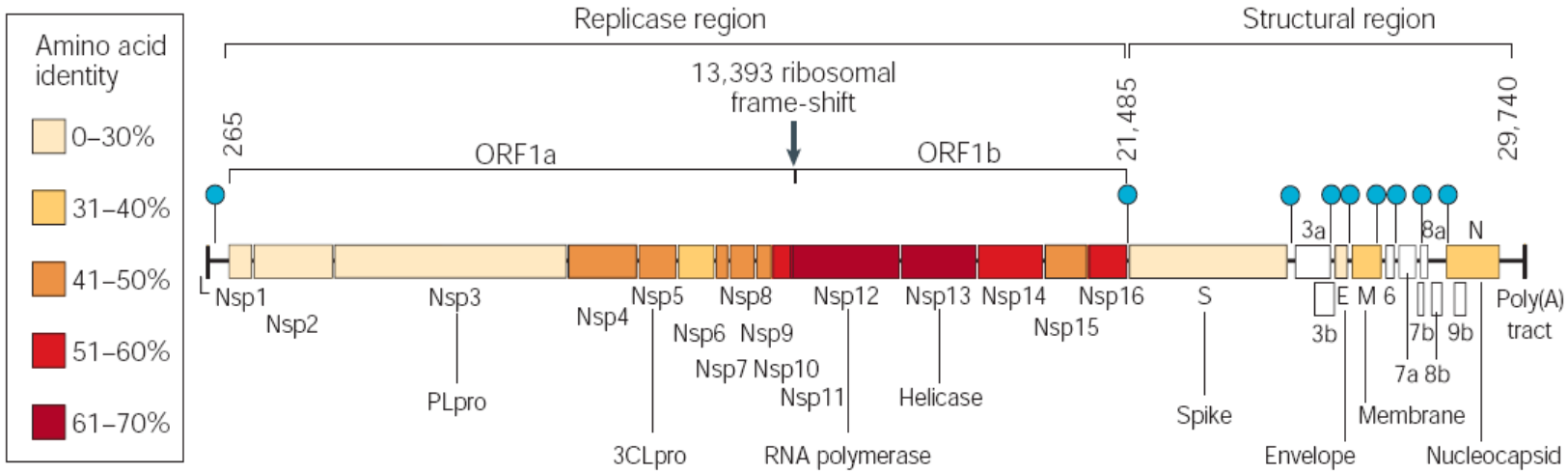

Figure1.3. Schematic represents SARS-CoV genomic organization.
SARS-CoV genome starts with leader sequence, subgequently are ORF1a and ORF1b, which are encode for polyproteins 1a and 1ab that will be cleaved into 16 small, functional proteins(. Relative regions encoding for SAR-CoV structrural protein and accessory proteins are also present. Blue color represents for translation regulatory sequence. Color represents the identity sequence with other coronaviruses. Nsp: non-structural proteins (Stadler *et.al.* 2003)

SARS-CoV synthesizes nine species of subgenomic mRNAs (Fig.1.4) (Marra *et.al.,* 2003; Rota *et.at.,* 2003; Thiel *et.al.,* 2003). The largest is the subgenomic mRNA 1 with the size equivalent to the genomic RNA and the smallest is mRNA 9 containing only two overlapping ORFs. All structural proteins of SARS-CoV are synthesized from different subgenomic mRNAs and their ORFs are the 5' most ORF of the sequence. Some subgenomic mRNAs of SARS-CoV are predicted to code for multi-proteins. For example, the subgenomic mRNA 3 is predicted to encode protein 3a and 3b; the subgenomic mRNA 7 encodes protein 7a and 7b; the subgenomic mRNA 8 encodes 8a and 8b and the subgenomic mRNA 9 encodes N protein and protein 9b (Marra *et.al.,* 2003; Rota *et.at.,* 2003; Ziebuhr, 2004).

Another unique structure of coronaviruses is the presence of the leader sequence in all subgenomic mRNAs (Spaan *et.al.*, 1983, Chang *et.al.,* 1994). All the sugenomic mRNAs of coronaviruses are capped at the 5' terminus (Lai and Cavanagh, 1997). These two elements play important role in translation of subgenomic mRNAs by cap dependent mechanism.

In SARS-CoV, the negative strand RNAs have complementary sequence with the sugenomic mRNAs and have sizes equivalent to each species of subgenomic mRNAs. It is believed now that negative strand RNAs are used as templates for synthesizing subgenomic mRNAs.

1.7. Transcription mechanism of SARS-CoV

SARS-CoV shares the common transcription mechanism with other coronaviruses. In fact, the 3' UTR of SARS-CoV can act as a cis-acting element for

genomic replication in murine coronavirus (Goebel *et.al.,* 2004). Transcription mechanism of coronaviruses followed a discontinuous mechanism and is directed by the 5' leader sequence, the 5' UTR and 3' UTR (Raman and Brian, 2005; Zhang *et.al.,* 2005). There are two models proposed for the discontinuous transcription mechanism of coronaviruses.

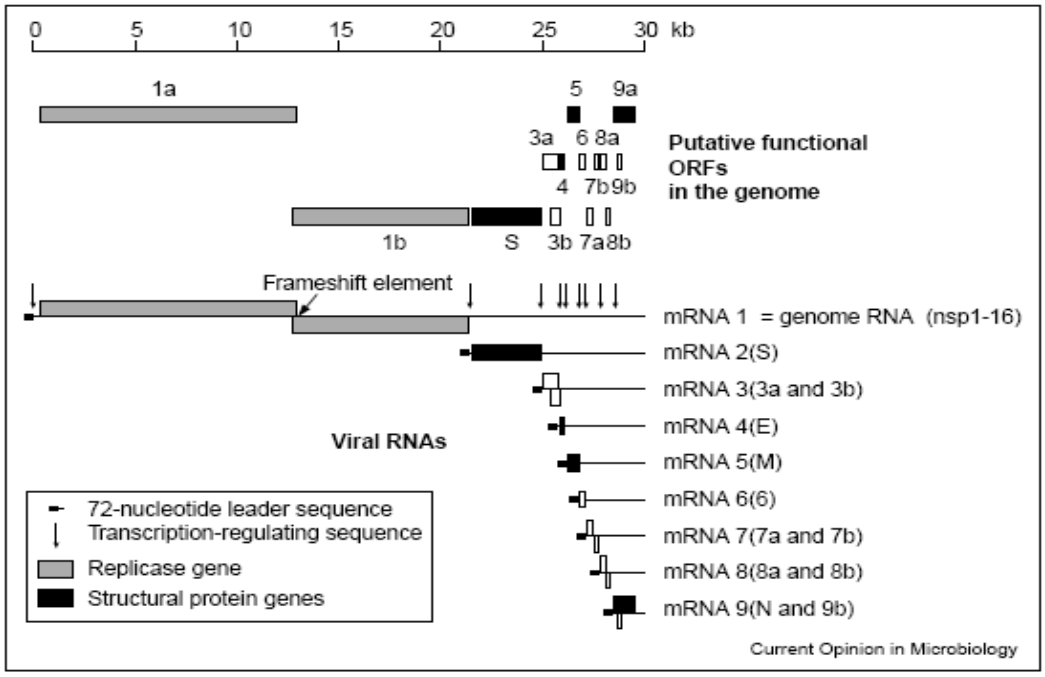

Figure 1.4. Diagram of subgennomic mRNAs of SARS-CoV
Nine species of subgenomic mRNAs of SARS and their predicted encoded proteins are relatively descrided (Ziebuhr, 2004).

One of the models relates to the priming of leader sequence. The leader sequence serves as primer for the synthesis of subgenomic mRNAs; the full-length negative strand RNA is used as a template to synthesize the different species of subgenomic mRNAs. The synthesized leader sequence was paired with the full-length negative strand RNA and initiates the transcription to synthesize subgenomic mRNAs. Subgenomic mRNAs in turn are used as the template to synthesize the negative strand RNAs (Lai and Cavanagh, 1997).

The current model relates to the negative strand RNAs which are used as template for the synthesis of subgenomic RNAs (Schaad and Baric, 1994; Sawicki and Sawicki, 1998; Marle *et.al.,* 1999). In this mechanism, the synthesis of each negative strand RNA species is separated into three steps (Sawicki and Sawicki, 1998). First, a complex forms between the 5' most TRS of the genome and the genomic 3' end, initiating the generation of nascent negative strand RNA. Second, the complex scans through the genomic RNA and synthesizes the negative strand RNA. Finally, when the complex scans through a TRS on the genomic RNA, it may switches the template to the leader sequence of the genome to generate the complementary leader sequence and then release negative strand RNA. There is increasing evidence proving that the discontinuous transcription mechanism of coronaviruses is followed this model (Sawicki and Sawicki, 1990; Zuniga *et.al.,* 2004).

1.8. Translation mechanism of SARS-CoV

The first two proteins synthesized are polyprotein 1a and 1ab (Ziebuhr *et.al.,* 2000). The translation of ORF1b is by a frameshifting mechanism (Brierley *et.al.,* 1987 Brierley *et.al.,* 1989), resulting in the generation of the fusion polyprotein 1ab. Polyproteins 1a and 1ab are then cleaved by two viral proteases embedded in these two polyproteins. The released proteins assemble together with host proteins to form replicase complex to synthesize negative strand RNA and subgenomic mRNAs and genomic RNA (Ziebuhr *et.al.,* 2000).

Most SARS-CoV proteins are translated by a cap dependent translation mechanism. Leader sequence and the cap at the 5' terminus present at each subgenomic

mRNA can form complex binding to ribosome (Tahara *et.al.,* 1994). Ribosome scans through subgenomic mRNA and starts translation at the first AUG encountered.

Some SARS-CoV accessory proteins are translated from the polycistronic mRNAs. Mechanism of translation of these proteins has yet to be elucidated. For example, protein 3b is predicted to be generated by internal ribosomal entry mechanism. Protein 7b and 9b are predicted to be generated by a leaky scanning mechanism (Snijder *et.al.*2003). Generation of protein 8b is not clearly understood.

1.9. Characterization of SARS-CoV protein

1.9.1. The polyprotein 1a and polyprotein 1ab

The polyprotein 1a and 1ab of SARS-CoV are generated as precursor proteins and subsequently were cleaved into 16 small and functional proteins (Ziebuhr, 2004).

Unlike other coronaviruses with the presence of two papain-like proteases (PLpro) 1 and 2 in the polyproteins, SARS-CoV has only one single PLpro (Nsp 3). It cleaves the N proximal region of 1a and 1ab at 3 sites and releases non-structrual proteins (Nsp) 1 and 2 and itself from precursor polyproteins (Fig.1.3) (Thiel *et.al*., 2003; Harcourt *et.al.,* 2004). PLpro may also have deubiquitin activity (Barretto *et.al.,* 2005).

Another protease also present in the SARS-CoV polyprotein is the 3C-like proteinase (Nsp 5) (Fan *et.al.,* 2004), which is a well characterized and highly conserved protein in coronaviruses. It is responsible for the cleavage of the remaining part of the polyproteins at 11 sites from Nsp 4 to Nsp 16 (Fig.1.3) (Thiel *et.al*., 2003). RNA dependent RNA polymerase (RdRp) of SARS-CoV is Nsp 12 and helicase is Nsp13 (Marra *et.al.,* 2003; Rota *et.al.,* 2003; Xu *et.al.,* 2003). These two proteins are highly

conserved in coronaviruses and are used as criteria to construct the unrooted and rooted phylogenetic tree of SARS-CoV. Together with other cleavage products, RdRp and helicase proteins are essential for the replication and transcription of SARS-CoV.

Structural studies have shown that Nsp 8 is able to interact with both Nsp 7 and Nsp 9 (Zhai *et.al.,* 2005). The super-complex forming between Nsp 7 and Nsp 8 interact with double strand RNAs and it encloses and stabilizes the RNA. Nsp 9 has structure similar to two subdomains of the SARS-CoV 3C-like proteinase and is supposed to evolve from a protease. Nsp 9 alone is able to bind to RNA (Sutton *et.al.,* 2004). These proteins together with RdRp and helicase therefore are predicted to involve in forming the replication and transcription machinery of SARS-CoV.

Nsp 10 interacts with the cellular oxido-reductase systems, causing extensive cythopathic effect (Li *et.al.,* 2005c). Nsp 14, Nsp 15 and Nsp 16 are predicted functionally as the exonuclease, endoRNAse and mRNA cap-1 methyltransferase, respectively (Stadler *et.al.,* 2003). However, their functions are not determined in infected cells. The rest of Nsps are with unknown function at present.

1.9.2. Characteristic of structural proteins of SARS-CoV

1.9.2.1. Spike (S) protein

S protein is one of the most well characterized proteins of SARS-CoV. It has a pental shaped structure, and is evenly projected on the lipid bilayer envelope, giving SARS-CoV a crown-like appearance. S protein is a class I fusion protein and is highly glycosylated with 23-predicted glycosylated sites (Bosch *et.al.*2003; Hofmann and Pohlmann 2004, Xiao *et.al.,* 2003).

S protein is responsible for the binding of SARS-CoV to host cellular receptor. One of the well-defined receptors of SARS-CoV is a metallopeptidase, angiotensin-converting enzyme 2 (ACE2) that is a carboxypeptidase functioning as a polypeptidase enzyme from the renal angiotensis system (Li *et.al.,* 2003; Hofmann and Pohlmann, 2004). ACE 2 is expressed in a variety of tissues and organs, permitting wide spread of SARS-CoV in human body (Li *et.al.,* 2005b; Hofmann *et.al.,* 2004). Another possible receptor reported to bind to the SARS-CoV S protein is the dendritic cell-specific ICAM-grabbing non-integrin (DC-SIGN) protein which is found on dendritic cells (Yang *et.al.,* 2004).

In other coronaviruses, S protein is cleaved into two domains S1 and S2 by the host cellular enzyme furin (Lai and Cavanagh, 1997). However, sequence alignment of murine hepatitis virus S protein with SARS-CoV showed the lack of essential residues for cleavage by furin. It is therefore likely that the SARS-CoV S protein is not cleaved into two domains by furin (Yao *et.al.,* 2004). Based on its functional similarity to the S protein of other coronaviruses, SARS-CoV S protein is theoretically divided into two functional domains S1 and S2 (Li *et.al.,* 2005b).

The S1 region is composed of 600 amino acids ranging from residue 12 to- 612. It is functionally divided into N terminal domain (12-306) and ACE2-receptor binding domain (306-667) (Wong *et.al.*2004). Structural studies showed that a gentle concave of an extended loop of S receptor binding domain cradles the N-terminal lobe of ACE 2 (Prabakaran *et.al.,* 2004; Kuba *et.al.,* 2005). Fourteen residues of this loop interact with 18 residues in ACE 2. Asparagine at position 479 and threonin at position 487 in S protein are two important residues involved in the specific binding to human ACE 2 (Li

et.al., 2005b). The receptor binding region of S1 (400-600) overlaps with a neutralizing epitope of S protein; and the neutralizing antibody against S protein blocks the binding of S protein to its receptor (Yi *et.al.,* 2005; Chen *et.al.,* 2005).

The S2 region is from amino acid residue 667 to 1190 and functions as a fusion domain. It characterizes S proteins as class I fusion protein with a fusion peptide, two heptad regions and a transmembrane domain. The transmembrane domain anchors S protein on the viral envelope. Upon binding of S protein to ACE2, conformational change of the coil – coil structrure brings the virus membrane coming into close proximity to host cell membrane and simultaneously exposes fusion peptide to insert to host cell membrane triggering the fusion of two membranes (Ingallinella *et.al.,* 2004; Tripet *et.al.,* 2005;). S protein of SARS-CoV mediate membrane fusion in means of pH-independence (Yang *et.al.,* 2004)or dependence (Simmons *et.al.,* 2004) leading to direct release of the genomic RNA into the cytoplasm of host cells (Zhang and Yap, 2004; Smith and Helenius, 2004) or direct the internalization of SARS-CoV using cellular endocytosis (Dimitrov, 2004). Schematic diagram representing the domains of SARS-CoV S protein is described in Fig.1.5.

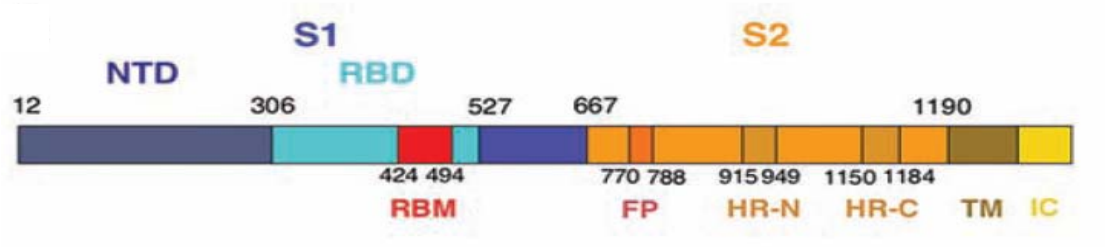

Figure1.5. Schematic diagram of S protein domain.
NTD: N terminal domain. RDB: Receptor binding domain. RBM: Receptor binding motif. FP: Fusion peptides. HR-N: N and HR-C: Heptad repeated region.. TM: Transmembrane domain. IC: Intracellular domain (Li *et.al.,* 2005b)

1.9.2.2. Envelope (E) and membrane (M) proteins

E and M proteins are two major components of the virus envelope. Association of E protein and M protein is essential for the assembly of virus-like particles (VLPs). When coexpressed in cells, M and E protein of SARS-CoV were able to form sedimentable particles. Location of these two proteins in the ER, Golgi and intermediate compartments is essential for the assembly and secretory of virus particles through the secretory pathways of cells. The ratio of E and M required for virus-like particle formation is 1: 5 (Huang *et.al.,* 2004a; Ho *et.al.,* 2004).

M protein is a glycosylated protein comprising of 221 amino acids; it forms three transmembrane helices domain from residues 15 to 99, and 121 amino acid hydrophilic domain on the inside of virus particles (Marra *et.al.,* 2003).

E protein is indispensable in the assembly of VLPs. It is a small protein with 76 amino acids. SARS-CoV E protein is less similar to other coronavirus envelope proteins (Aebely *et.al.,* 2004).

1.9.2.3. Nucleocapsid (N) protein

SARS-CoV N protein consists of 422 amino acids and is minimally homologous to other coronavirus proteins. It is essential for the packing of RNA genome. Two independent RNA binding domain of N protein are located at the N- and C-terminal regions of the protein. Deletion of these two domains diminishes RNA binding capability of N protein. During packaging, N protein binds to specific RNA sequence of the genomic RNA located the 3' terminal region of ORF1b (Huang *et.al.,* 2004b).

N protein of SARS-CoV is localized mainly to the cytoplasm and some is found in the nucleus (You *et.al.,* 2005; Rowland *et.al.,* 2005). The protein is capable of forming dimers and high order multmers. A small ubiquitin-like modifier (SUMO) is reported to attach covalently to N protein at lysine residue 62 (Li *et.al.,* 2005b). The binding of SUMO to N protein promotes homo-oligomerization of the protein. N protein is also reported to be cleaved by caspase 3; it induces T-cell response and it activates activator protein 1 signal transduction pathway. N is implicated to induce the host immunoresponse through the activation of nuclear factor kappa B (NFκB) protein (Tan *et.al.,* 2005; Liao *et.al.,* 2005) .

1.9.3. Characteristics of SARS-CoV putative proteins

SARS-CoV encodes a unique set of ORFs which do not share with any of the known coronaviruses. They are ORF 3a, 3b, 6, 7a, 7b, 8a, 8b and 9b, which are predicted to encode accessory proteins of SARS-CoV. Among these SARS-CoV accessory proteins, protein 3a, 7a, 8a and 9b have been detected in patients sera (Guo *et.al.,* 2004; Qiu *et.al.,* 2005b; Tan *et.al.,* 2004a).

In other coronaviruses, some subgroup-specific accessory proteins are dispensable for viral replication, at least in cell culture system. They may have important role in interaction between host and virus, thus contributing to viral fitness (Brown *et.al.,* 1995; Lai and Cavanagh, 1997).

Some of SARS-CoV accessory proteins have been characterized. One of the well characterized accessory proteins of SARS-CoV is protein 3a. It is encoded by ORF3a on subgenomic mRNA 3 and is the largest accessory protein of SARS-CoV. Expression of

protein 3a is detected in patients' lung specimen as well (Yu *et.al.,* 2004; Zeng *et.al.,* 2004; Tan *et.al.,* 2005b). Protein 3a is located in the perinuclear region and Golgi apparatus and it interacts with structural proteins S, M and E (Qiu *et.al.,* 2005; Yuan *et.al.,* 2005a). In addition, it is transported to the surface of host cells and undergoes endocytosis (Tan *et.al.,* 2004d). Protein 3a is found to stimulate the expression of fibrinogen (Tan *et.al.,* 2005e). Protein 3a is proposed as a novel structural protein (Shen *et.al.,* 2005) and is shown to induce apoptosis in Vero E6 cells (Law *et.al.,* 2005).

Protein 3b of SARS-coV is also studied. It is encoded by ORF3b. Protein 3b is a 154 amino acid protein and is localized to the nucleus (Yuan *et.al.,* 2005c). It induces cell cycle arrest at G0/G1 phase (Yuan *et.al.,* 2005b). The protein is predicted to be translated by an internal ribosomal entry mechanism. (Siijder *et.al.,* 2004)

Protein 7a is encoded by ORF7a of the subgenomic mRNA 7 and is composed of 122 amino acids. It is likely a type I membrane protein (Nelson *et.al.,* 2005; Bartlam *et.al.,* 2005). Its C-terminal tail contains a typical ER retrieval motif. Protein 7a is located in the perinuclear region in SARS-CoV infected cells (Fielding *et.al.,* 2004). Overexpression of the protein induces apoptosis in different cell lines via a caspase-dependent pathway (Tan *et.al.,* 2004c).

Characteristics of the rest accessory proteins of SARS-CoV have not been elucidated yet. For example, protein 6 is predicted as a 63 amino acid protein encoded by the sugbenomic mRNA 6. It is predicted as a transmembrane protein of the viral envelope with N terminal outside of VLPs (Marra *et.al.,* 2003). Protein 7b is predicted as a 44-amino acid protein. It is encoded by ORF7b of the subgenomic mRNA 7 (Marra *et.al.,* 2003).

Protein 9b is downstream of N protein in subgenomic mRNA 9. It is 98-amino acid protein and is predicted to be expressed as leaky scanning of ribosome (Snijder *et.al.,* 2003).

1.9.4. The putative protein 8a, 8b and 8ab of subgenomic mRNA 8 of SARS-CoV

Protein 8a and 8b are encoded by two overlapping ORFs (8a and 8b) of the subgenomic mRNA 8. In fact, the subgenomic mRNA 8 of most SARS-CoV strains collected from human isolates at the late stage of the outbreak is found with 29-nucleotide deletions (between T_{27867} and A_{27868} for strain SG2774 (accession No: AY283798)) and two overlapping ORFs 8a/b (Marra *et.al.,* 2003). In contrast, the subgenomic mRNA 8 of most SARS-CoV strains collected in animal and in human isolates at the early stages of epidemic and is found with a single ORF 8 (Guan *et.al.,* 2003). ORF 8 is predicted to encode a single protein 8ab, a fusion form of protein 8a and protein 8b. The deletion of 29 nucleotides and the formation of two ORFs of SARS-CoV are predicted as the adaptation of SARS-CoV from animals to human (Guan *et.al.,* 2003; Poon *et.al.,* 2004. Lau *et.al.,* 2005; Li. *et.al.,* 2005). The schematic diagram of the SARS-CoV genome with and without the 29 nucleotides is described in Fig 1.6.

ORF 8a and ORF 8ab are located immediate downstream of a strong TRS (AGUCUAAACGAA**AUG**) (Snijner *et.al.,* 2003). Protein 8a contains 39 amino acids is predicted as a secretory protein containing a secretory signal sequence at the N-terminal region. Protein 8ab consists of 122 amino acids (Marra *et.al.,* 2003).

Protein 8b consists of 84 amino acids. The splitting of ORF 8 into two overlapping ORF 8a/b due to the 29-nucleotide deletion makes it difficult to understand

the translation mechanism of ORF 8b. In fact, ORF 8b is located downstream of a weak TRS in the subgenomic mRNA 8a/b (CUAAUAAACUC**AUG**) (Marra *et.al.,* 2003), but no additional sugenomic mRNA of SARS-CoV is found. Protein 8b and antibodies against this protein are not detected in infected patients. Protein 8b is predicted as a glycosylated protein (Rota *et.al.,* 2003; Marra *et.al.,* 2003; Guan *et.al.,* 2003).

The expression of these ORFs together with characteristics of proteins encoded by subgenomic mRNA 8 is presented in detail in chapter 3.

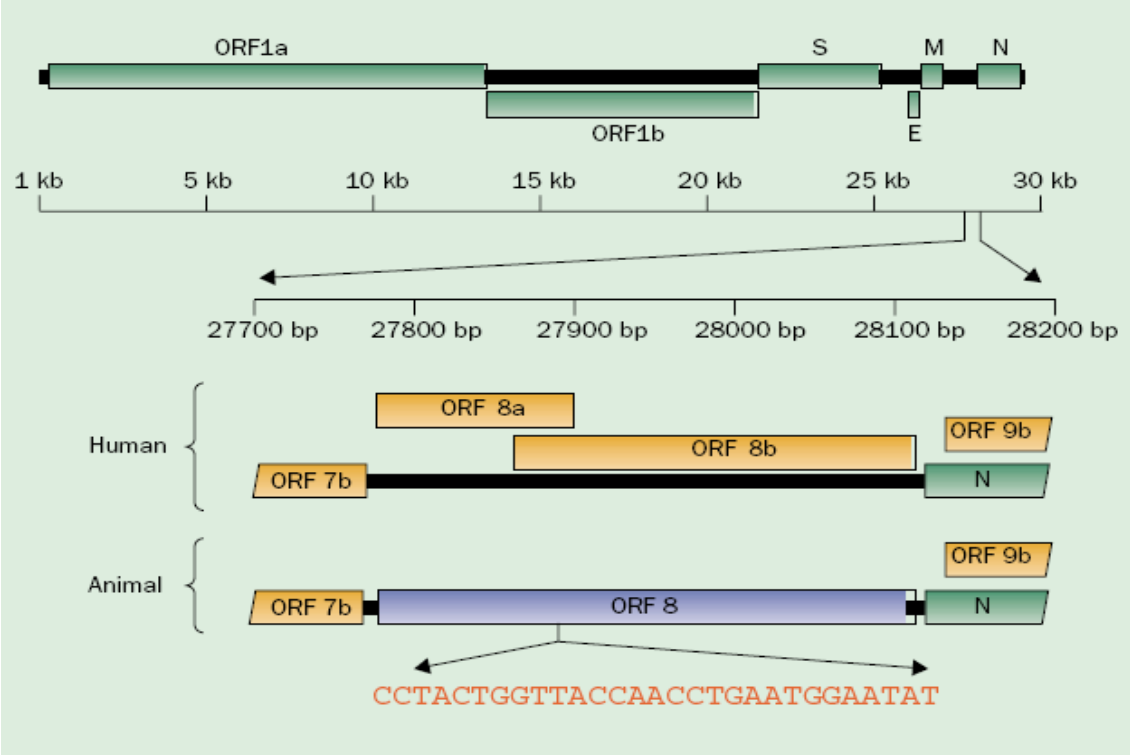

Figure 1.6. Diagram of 29 nucleotide deletion of sugenomic mRNA 8 (Poon *et.al.,* 2004).
a. Genomic organization of SARS-CoV isolated from human and animal. ORF1a and ORF1b encode for polyprotein 1a and 1ab, followed by the regions encoding for structure protein S, E, M and N. These regions are illustrated in green boxes.
b. Expanded view from nucleotide 27700 to 28200 of the SARS-CoV genomic sequence (based on AY278554 numbering). Putative ORFs in this region were indicated by brown boxes. The presence of 29-nucleotide sequence in ORF 8 from residue 27868 was described. Deletion of 29 nucleotides results in the splitting of ORF 8 into two ORFs - ORF 8a and ORF 8b in human isolates at the late stage of epidemic.

1.10. The life cycle of SARS-CoV

The detailed life cycle of SARS-CoV has not been fully investigated. Generally, a coronavirus replication cycle comprises the following steps: viral attachment to host cell membrane receptor, penetration and uncoating of virus particles into cells, synthesis of genomic and subgenomic RNA, production of viral proteins in the cytoplasm, assembly in the ER and Golgi and release viral particles from cells (Lai and Canavagh, 1997; Lai and Holmes, 2001).

Under microscope, SARS-CoV was observed to enter Vero E6 cells by membrane fusion between its envelope and host cellular membrane. The assembly of virion is started by the accumulation of RNPs in the swollen round ER and Golgi apparatus. Virions are released by smooth vesicles (Qinfen *et.al.,* 2004).

At the molecular level, SARS-CoV life cycle starts when the viral S protein interacts with host cell membrane receptors (Yang *et.al.,* 2004), resulting in the release of viral genomic RNA. Once in the host cytoplasm, the RNA genome is translated by host translation mechanism to generate polyproteins 1a and 1ab. These polyproteins are cleaved by themselves into smaller proteins to form the special replicase machinery. This replicase machinery in turn synthesizes the genomic and negative strand RNA from genomic RNA templates. The subgenomic mRNA is synthesized from negative strand RNA. Through the transcription and translation of the subgenomic mRNAs, the structural proteins and other accessory proteins of SARS-CoV are synthesized.

Currently, details of the assembly process of SARS-CoV is not clear. However, in MHV, the viral assembly started with package of the genomic RNA into nucleocapsid. Efficient package of SARS-CoV genomic RNA requires the specific RNA signal that is

predicted to consist of a 70-nucleotide stretch at the 3' terminus of the ORF 1b (Huang *et.al.,* 2004b). The N protein without the genomic RNA is unable to package into virions. Once the ribonucleocapsid is formed, it interacts with the M protein (Ho *et.al.,* 2004). The interaction between M and ribonucleocapsid complex may lead to the formation of spherical internal core shell surrounding the ribonucleocapsid. Virus particle formation takes place at the ER or Golgi membrane where M and E protein are anchored (Ho *et.al.,* 2004; Nal et.al., 2005). Virion release is mediated by host secretory pathway.

1.11. Scope of thesis

SARS-CoV contains group-specific ORFs which are not homologous to any proteins from other coronaviruses. These ORFs all encode SARS-CoV accessory proteins. In other coronaviruses, accessory proteins are predicted to contribute to the fitness of virus to adapt to host.

In SARS-CoV, the most striking difference is found with the 29-nucleotide deletion in the subgenomic mRNA8 of SARS-CoV isolated from human patients at the late stage of the outbreak. This deletion results in splitting of a single ORF (ORF 8) into two ORFs (ORF 8a and 8b) and is predicted to attribute to the adaptation of SARS-CoV from animals to human.

ORF 8a and 8b are predicted to encode two small proteins, 8a and 8b, and ORF 8 a single protein 8ab (a fused form of 8a and 8b proteins). To understand the functions of these proteins, cDNA fragments covering these ORFs were cloned into expression plasmids, and expressed in *in vitro* and *in vivo* systems. It was shown that expression of a construct containing ORF 8a and 8b generated only a single protein 8a; no detection of the 8b expression was obtained. Expression of a construct containing ORF 8 generated

the 8ab fusion protein. Subcellular localization studies of HeLa cells expressing 8a, 8b and 8ab proteins showed that protein 8a and 8ab are localized to the cytoplasm and protein 8b in the ER. Site-directed mutagenesis and enzymatic treatment revealed that 8b and 8ab were modified by N-linked glycoprotein, and by ubiquitination. More interestingly, the two proteins could form complex with ubiquitin and interferon regulatory factor 3, suggesting the potential involvement of these protein in the pathogenesis of SARS-CoV.

CHAPTER 2. GENERAL MATERIALS AND METHODS

2.1 General materials

2.1.1. Plasmids

Cloning plasmids used in this project:

pKT0 and pKT-Flag (Liu *et.al.*1994) contain T7 promoter. Protein expression using these constructs was dependent on the Vaccina/T7 system to provide the T7 polymerase.

pXJ40 were made by contains with human cytomegalovirus (CMV) IE promoter, and could be expressed in mammalian cells.

pGEX-5X-1 (Amersham) was used to express Gluthionine S-transferase (GST) fused protein in *Escherichia coli* (*E.coli*).

p53 were cloned by Prof. David Lane' lab (IMCB). IκBα were cloned by Dr.Vinay Tergaonkar's lab(IMCB). pMyc- Ubiquitin (pMyc - Ubi) were cloned by Dr. Daoxin Xie(IMCB). These three plasmids contain CMV IE promoters.

2.1.2. Antibodies

Primary antibodies: anti-Flag and anti-Myc monoclonal antibodies were from SIGMA; anti-IRF3 and anti-I kappa B alpha (IκBα) antibodies were from Santa Cruz; anti-p53 antibodies were from David Lane's lab and anti-8b antibodies were raised in rabbits in our lab.

Secondary antibodies: goat anti-mouse secondary antibodies conjugated with horseradish perosidase (HRP), and mouse anti-goat or anti-rabbit secondary antibodies

conjugated with HRP were purchased from DAKO. Goat anti-mouse or goat anti-rabit secondary antibodies conjugated with flourescein isothiocyanate were from Invitrogen.

2.2. Cloning and DNA manipulation

2.2.1. DNA plasmid purification

2.2.1.1. Alkaline lysis for plasmid screening

Single colonies of bacteria were inoculated into 1.5 ml of Luria-Bertani [10 g tryptone, 5 g yeast extract and 10 g NaCl in 950 ml sterile water] with 1 µg/ml ampicillin (LB/ampicilin) and cultured at 37^{o}C overnight. The culture was centrifuged at 13000 rpm at room temperature (RT) for 1 min. The supernatant was removed, and pellets were resuspended in 140 µl of Solution I [50 mM sucrose, 25 mM Tris-HCl (pH 8), 10 mM ethylene diamine tetra-acetic acid (EDTA)], followed by lysis with 140 µl of Solution II [200 mM NaOH, 1 % SDS] and then neutralized with 200 µl of Solution III [3 M MaOAc pH5.2]. Samples were centrifuged at 13000 rpm for 5 min. The supernatant was transferred to a tube containing 2 volume of absolute ethanol, followed by vortexing and incubation at RT for 10 min. The precipitated DNA was collected by centrifuging at maximum speed for 5 min and resuspended in 50 µl sterile water.

2.2.1.2. Qiagen midipreps

A single colony was inoculated in 3 ml 1 X LB/ampicillin and cultured at 37^{o}C overnight. DNA purification was performed according to the manufacturer's instructions. Ten micrograms of DNA was purified.

2.2.1.3. Promega midipreps

Five to eight colonies were inoculated in 50 ml LB/ampicillin. Using the Promega midiprep kit, 120 – 180 µg of DNA was purified from 50 ml overnight bacterial culture according to the manufacturer's protocol.

2.2.2. DNA concentration determination

Four micro-liters of DNA preparation were diluted 1:200 in distill water. Spectrophotometric readings of DNA at A_{260nm} and A_{280nm} were taken. One OD_{260nm} is equivalent to 50 µg DNA per µl. The ratio A_{260nm} to A_{280nm} is used to determine DNA purity.

2.2.3. Polymerase chain reaction (PCR)

Specific primers were designed manually. In each PCR reaction, appropriate primers and DNA templates were used together with Tag P*fu* DNA polymerase (Fermentas). Components for 50µl reaction were mixed as follows:

DNA template (0.2µg/µl)	0.5 µl
NTPs (10 mM each of dATP, dGTP, dCTP, dTTP)	1 µl
10 X Tag or P*fu* DNA reaction buffer	5 µl
Forward primer (10pmol/µl)	1 µl
Reverse primer (10pmol/µl)	1 µl
Tag polymerase or P*fu* DNA polymerase (2U/µl)	2 µl
Sterile water to final volume of 50 µl	

The PCR conditions were carried out at 95°C for 5 min, followed with 35 cycles of denaturing at 95°C for 45 sec, annealing at 50 – 55°C for 45 sec, elongation at 72°C for 1 min and a final elongation 72°C for 10 min. On completion of the PCR program, the samples were cooled to 16°C.

2.2.4. Overlapping PCR

Overlapping PCR was used to get chimera PCR fragment using a two steps PCR approach as described in Fig. 2.1.

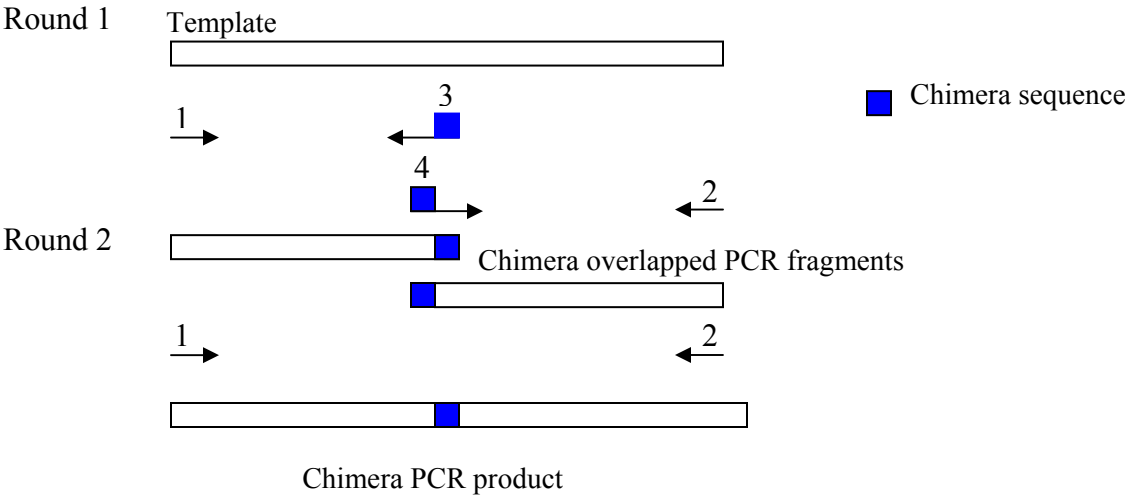

Figure 2.1. Overlapping PCR Legend

The overlapping PCR contained 2 set of primers as shown above. Primer 3 and 4 were designed to have an overlapping chimera sequence. The first step involved two PCR reaction with a common template using two different sets of primers : primers 1/ 3 and primers 2/ 4. The second round used the two chimera overlapped PCR fragments as templates together with primers 1 and 2. The PCR conditions of each round were the same as in outlined in 2.2.3.

2.2.5. Site-directed mutagenesis

A set of complementary primers bearing nucleotide mutations was designed to synthesize the mutant plasmid. PCR was performed with P*fu* turbo polymerase (Stratagene). Components in each PCR reaction were mixed as in normal PCR. The PCR conditions were: 95^{o}C for 5 min followed with 12 - 16 cycles of 95^{o}C for 45 sec, 50 – 55^{o}C for 45 sec and 68^{o}C for 3-5 min and cooled to 16^{o}C. The elongation times were adjusted accordingly to the length of plasmid DNA.

Fifty micro-liters of PCR samples were digested with 1 µl Dnp I (New England Biolabs). Subsequently, 1 µl of digested PCR samples was directly transformed into *E.coli* DH5α, spread onto 1.5 % agar LB/ampicilin plate and incubated at 37^{o}C overnight. DNA plasmids were extracted using Qiagen midipreps. The correct plasmid was verified by automated sequencing with appropriate primers.

2.2.6. Automated DNA sequencing

Two hundred nanograms DNA was added to a mixture containing 10 pmol of primer, 4 µl of big dye termination (ver. 3.1) reaction mix and sterile water in the 10µl reaction.

The sequencing conditions were 96^{o}C for 10 sec, 50^{o}C for 5 sec, and 65^{o}C for 4 min for 25 cycles and cooled to 16^{o}C.

The sequenced product was then purified to remove any residual dye. The sequenced product was precipitated with 80µl of 80% ethanol, vortexed briefly and incubated at room temperature for 20 min. The mixture was centrifuged at 13000 rpm for 15 min. The supernatant was discarded and the pellet was washed with 150 µl of 70%

ethanol by centrifuging at 13000 rpm for 5 min. The supernatant was removed and the pellet was vacuum dried for 8 min. The sequence was determined on an Applied Biosystems Model 3730XL automatic DNA sequencer at the DNA Sequencing and Analysis Facility in (IMCB).

2.2.7. Agarose gel electrophoresis and gel purification

One percent agarose gel was prepared by dissolving agarose powder (Invitrogen) in 1 X TAE (40 mM Tris-acetate, 1 mM EDTA) buffer and 0.5 μg/ml ethidium bromide (SIGMA). The DNA samples were mixed with 6 times loading dye (0.25 % bromophenol blue, 0.2 5% xylene cyanol FF and 40 % sucrose in sterile water) in the ratio 5: 1 before loading into individual wells. The Gel was submerged in a running tank (Hybaid) of TAE buffer and run horizontally at 120 Volts (Hoeffer Scientific Instruments) at constant voltage. Nucleic acid bands separated on agarose gels were visualized by UV transillumination (BIORAD), and fragment sizes were compared with a 1 kb ladder DNA marker (Gibco BRL).

For gel purification, upon separation and viewing, the desired band was excised. Purification of DNA fragment was achieved using Qiagen gel extraction kit according to manufacturer's instructions.

2.2.8. PCR Purification

PCR products were purified using Qiagen PCR clean up kit according to the manufacturer's instruction.

2.2.9. Restriction endonuclease digestion

Two micrograms of DNA plasmid or PCR fragment were mixed with 10 units of appropriate restriction enzymes (New England Biolabs or Promega) in a 25 µl of reaction buffer and digested for 1.5 hrs at the recommended temperature by the manufacturer. For double digestion, the reaction was digested concurrently for 1.5 hrs at the manufacturer's recommended temperature.

2.2.10. Dephosphorylation of vector

Dephosphorylation of digested plasmid was done with Calf intestinal phosphatase (CIP) from New England Biolabs. Two smicrograms of digested plasmid DNA was mixed with 1 U of CIP in 50 µl reaction. After incubation at 37^{o}C for 1 hr, the DNA was extracted by Qiagen PCR clean up kit.

2.2.11. Ligation of DNA insert and vector

The Ligation was carried out in a 20 µl reaction. Purified, dephosphorylated vector and appropriate excised DNA insert were mixed in a ratio 1:3 in the presence of 1 U of T4 DNA ligase (New England Biolabs) in recommended buffer. The mixture was incubated at 16^{o}C overnight.

2.3. Bacterial transformation

2.3.1. Preparation of (*E.coli)* DH5α and BL21 competent cells for heat shock transformation

A single colony of *E.coli* DH5α or BL21 from 1.5 % agar was inoculated in 5 ml of liquid LB at 37^{o}C overnight. Four micro-liters of overnight culture was inoculated into 200 ml of LB and incubated at 37^{o}C until an OD_{660} of 0.6-0.8. The cells were cooled down on ice for 30min prior to centrifugation at 4000 rpm at 4^{o}C for 15 min. The cells were resuspended in 40 ml of ice-cold 0.1 M $CaCl_2$ and incubated on ice for 1 hr. After centrifugation, the cells were resuspended in 4 ml of ice-cold 0.1 M $CaCl_2$ and 20 % glycerol. The prepared competent cells were aliquoted into small vials and stored at -80^{o}C.

2.3.2. Heat shock transformation

One hundred nanograms of plasmid DNA or 5 µl ligated DNA were added to 50 µl of compatible competent cells, incubated on ice for 30 min, followed with incubation at 42^{o}C for 2 min and then on ice for 5 min.

Transformed bacteria were directly spread on 1.5% agar, LB/ampicilin plate and incubated at 37^{o}C overnight.

Bacteria transformed with ligated DNA were recovered by adding 1 ml of 2 X LB and incubated at 37^{o}C for 1 hr. 100 µl of bacteria were then spread on 1.5 % LB agar with ampicilin plate and incubated at 37^{o}C overnight.

2.4. Transcription and translation

2.4.1. Coupled in vitro transcription and translation

One microgram of plasmid DNA was mixed with TNT coupled wheat germ extracts or rabbit reticulocyte lysates in the presence of ^{35}S methionine according to the

manufacturer's instruction. The mixture was incubated at 30°C for 90 min and used for subsequent experiments or kept at -20°C.

2.4.2. Transient transfection of mammalian cells

Eighty to ninety percent of confluent monolayer of mammalian cells on 30-mm NUNC dishes was transfected with 4 μg of plasmid DNA using Lipofectamine 2000 reagent (Invitrogen) according to the manufacturer's instruction. Cells were grown in serum and antibiotics-free DMEM and incubated at 37°C with 5 % CO_2. After 4 to 6 hrs posttransfection, the medium was removed and replaced with fresh DMEM supplemented with 10 % FBS, 1 % ampicillin and 1 % streptomycin, and continuously incubated at 37°C, 5% CO_2 for 24 hrs. The cells were then washed once with sterile phosphate-buffer saline (PBS), harvested and kept at -20 °C until further analysis.

2.4.3. Transient transfection of mammalian cells using a recombinant vaccinia virus/T7 expression system

Eighty to ninety percent of confluent monolayer of mammalian cells on 30-mm NUNC dishes was infected with recombinant vaccinia virus that generated bacteriophage T7 RNA polymerase. After 4 hrs post-infection, the virus was removed. Cells were washed once with DMEM and transfected with 0.4 μg of plasmid DNA by using the effectene transfection reagent (Qiagen) according to the manufacturer's instruction. After incubation at 37°C, 5 % CO_2 for 18 hrs, the cells were washed twice with PBS and harvested for further analysis.

2.4.4. Induction of Gluthionine S-transferase (GST) - fusion protein expression in *E.coli* BL21 cells

Three single colonies of *E.coli* BL21 were inoculated in 1 0ml 1X LB/ampicilin at 37^{o}C overnight with shaking. Ten milliliters were used to inoculate in 1 liter of 2X LB and incubate at 37^{o}C. Until OD_{600nm} reached 0.6 - 0.8, the expression of the GST - fusion protein was induced with 1mM IPTG for 3 hrs. Each 100ml culture was centrifuged at 2500rpm for 20 min. Supernatant was removed and pellet was kept at -20^{o} C.

2.5. Cell manipulation

2.5.1. Labeling mammalian cells with ^{35}S methionine

At four hours post-transfection, cells were washed twice with methionine-free DMEM and starved in methionine-free DMEM for 30 min and then labeled with 25 mCi/ml [^{35}S] methionine. At 18 hr post-transfection, the ^{35}S labeled cells were washed twice with PBS and harvested with appropriate buffer.

2.5.2. Cell treatment with proteosome inhibitors

At 6 hrs post-transfection, each of 6 well-plate cells was changed with 2ml fresh DMEM. Ten micro-liters of lactacystin and 10 µl of 4-hydroxy-5-iodo-3-nitro-phenylacetyl-leucyl-leucyl-leucine vinyl sulfone (NLVS) were added to make the final concentration to 4 µM lactacystin and 8 µM NLVS. As these two proteosome inhibitors were dissolved in DMSO, 10 µl of DMSO and 10 µl of PBS were added to the control.

2.6. Protein manipulation

2.6.1. Treatment with PGNase F

Total cell lysates prepared from Cos-7 cells were directly treated with 4µl PGNAse F (New England Biolab) for 2 hrs at 37^{o} C. The sample was separated on 20% SDS-PAGE and analyzed by Western Blot with anti-Flag antibody.

2.6.2. Urea dialysis

One hundred mili-liters of the inducted bacteria culture were pelleted. The pellet was washed with 100 ml ice cold PBS in the presence of protein inhibitors from Roche. The washed pellet was resuspended in 60 ml of PBS with PI, and sonicated on ice. The sonicated sample was centrifuged at 12000rpm for 15 min.

Each pellet was added to 30 ml solution I [8 M Urea, 50 mM $NaHCO_3$ (pH 9), 1 mM DTT, 1 mM EDTA] and shaked at RT for 1 hr. The mixture was centrifuged at maximum speed for 15 min at RT. The supernatant was transferred to a dialysis tube (Pierce).

Dialysis was carried out at RT in 500 ml of solution II [4M Urea, 50mM $NaHCO_3$ (pH 9), 1 mM DTT, 1 mM EDTA] for 1 hr. Subsequently, the tube was dialyzed in 500 ml of solution III [2 M Urea, 50 mM $NaHCO_3$ (pH 9), 1 mM DTT, 1 mM EDTA] at 4^{o}C for 1 hr. This step was repeated once with fresh solution III. Next, the tube was dialyzed in 200 ml of solution IV [50 mM $NaHCO_3$ (pH 8.3), 1 mM DTT, 1 mM EDTA] at 4^{o}C for 1 hr. This tube then is dialysized in 500 ml of solutionV [50 mM $NaHCO_3$ (pH 9), 1 mM DTT, 1 mM EDTA] at 4^{o}C for 1 hr or overnight. The dialysized mixture was

centrifuged at maximum speed for 30 min. Supernatant was collected and kept at 4^{o}C for further analysis.

2.6.3. Prebinding protein to gluthionine sepharose beads

50 µl of gluthionine Sepharose beads (Amersham) was washed once with PBS and mixed with 600 µl of dialysized supernatant or sonicated supernatant of the culture expressing GST or GST fusion proteins. The complex was shook at room temperature for 30 min. The beads were then washed three times with PBS. The protein prebound beads were kept 4^{o}C for further experiments.

2.6.4. GST pull-down assay

Pull-down with the ^{35}S labeled cell lysate: 500 µl of ^{35}S methionine labeled cell lysate were incubated with 50 µl of GST prebound beads and incubated at 4^{o}C for 2 hrs. The mixtures were then centrifuged at 13000 rpm for 2 min in order to preclear non-specific binding proteins. The precleared supernatants were incubated with 30 µl of beads prebound with GST or GST-fusion proteins and incubated at 4^{o}C for 2 hrs. The beads were washed with RIPA buffer [50 mM Tris-HCl (pH 7.5), 150 mM NaCl, 0.5 % sodium deoxycholate, 0.5 % Nonidet P-40, 0.05 % SDS] for three times and resolved in SDS-PAGE. Protein bands were visualized with autography.

Pull-down with unlabeled cell lysate: cell lysate was directly mixed with beads prebound with GST or GST-fusion protein and incubated at 4^{o}C for 2 hrs. The beads were washed with RIPA buffer three times and resolved in sodium dodecyl sulfate-

polyacrylamide gel electrophoresis **(**SDS-PAGE). Western blot with appropriate antibodies was used to analyze results.

2.6.5. Immunoprecipitation

Transfected mammalian cells were washed one time with PBS, and lysed with 500 µl of RIPA buffer plus proteinase inhibitors (Roche). Cell debris was removed by centrifuge at 13000 rpm for 30 min at 4°C. The supernatant was incubated with 1 µg of appropriate antibodies for 2 hrs at room temperature with shaking. The mixtures were incubated with 50 µl protein A conjugated agarose beads (KLP) for 2 hrs. Subsequently, the beads were washed three times with RIPA buffer. The washed beads were added with 30 µl of 2 times Laemmli's sample buffer and were analyzed by Western blot.

For the ^{35}S labeled *in vitro* translation products, 10 µl of sample was lysed with 90 µl of RIPA buffer before the addition of appropriate antibodies.

2.7. Protein analysis

2.7.1. Sodium dodecyl sulfate-polyacrylamide gel electrophoresis (SDS-PAGE)

Discontinuous SDS-PAGE systems were carried out according to Laemmli's methodology. 5 % stracking gel and resolving gel of various concentrations (8 %, 10 %, 12 % and 20 %) were cast between two glass plates (BIORAD). Cell lysates or *in vitro* translation products were mixed with 2 X Laemmli's sample buffer [24 mM Tris.HCl (pH 6.8), 100 mM DTT, 2 % SDS, 0.1 % (w/v) bromoblue phenol, 20 % (v/v)glycerol]. The samples were boiled at 100^{o}C for 5 min and cooled on ice before loading on gel.

Gel system was dammed in tank with the running buffer [25 mM Tris-HCL, 192 mM glycine, 0.1 % (w/v) SDS, pH 8.3]. Gels were run vertically at constant current of 10 mA when the samples were in stacking gel and increased to 20mA when the samples were in the resolving gel.

2.7.2. Autography

SDS-PAGE gels for the ^{35}S methionine labeled samples were fixed in destaining buffer [50 % (v/v) methanol and 10 %(v/v) acetic acid] for 30 min. The signals on the gels were enhanced in Amplify solution (Amersham) for 15 min. Gel was dried at 80^{o}C for 1 hr and cooled at room tempearture for 15 min. Subsequently, the gel was exposed to X-Ray Film (Biomax, Kodak) for 2 days at - 80^{o} C.

2.7.3. Wet transfer

SDS-PAGE gels and polyvinyldifluoride (PDVF) membrane (BIORAD) were presoaked in 100 % methanol for a few seconds and were subsequently soaked with cold wet transfer buffer [25 mM Tris, 190 mM glycine, 20 % (v/v) methanol]. The SDS-PAGE gels, PDVF membrane and filter paper were assembled into the wet transfer cassette following the manufacture's instruction. The cassette was put into a reservoir filled with ice cold wet transfer buffer. The wet transfer was run at a constant voltage of 110 volts for 2 hrs, or at 55 volts for 16 hrs.

2.7.4. Western blot analysis

After the wet transfer, the PVDF membrane was blocked with 10 % skim milk for 1 hr followed by 1 hour incubation with appropriate primary antibodies. The membrane was washed for 10 min with PBST [PBS containing 0.1% (v/v) Tween 20] for five times. The membrane was continuously incubated with appropriate secondary antibodies conjugated with HRP for 1 hr. Subsequently, the membrane was washed five times with PBT for 10 min each interval. Proteins bound to membrane were detected by using ECL plus Western blot detection system buffer (Amersham).

When necessary, the membrane can be reincubated with another primary antibody after the signals were stripped with stripping buffer [2 % (v/v) SDS, 100 mM β-mercaptoethanol, 62.5 mM Tris-HCl, pH 6.8] for 30 min at 55^{o}C and washed extensively with PBST.

2.7.5. Coommassie blue staining

Protein separated on SDS-PAGE gels were stained with Coommassie blue [0.05 % Coommassie blue R-250 (SIGMA), 500 ml methanol, 100 ml acetic acid, 400 ml H_2O] for 30 min at room temperature with shaking. The gels were then destained with distaining buffer [500 ml methanol, 100 ml acetic acid, 400 ml H_2O] till protein bands on gels can be visualized clearly.

2.8. Microscopy and immunofluorescence

Mammalian cells were seeded on 4-well chamber slides (Iwaki) and grew for overnight. Cells were transfected with appropriate plasmid DNA cloned in pFlag (Liu

et.al. 1994) or pXJ40 (Xiao *et.al*.1991). At 18 hour normal post-transfection, the cells were rinsed with PBS, and fixed using 4 % (v/v) paraformaldehyde for 10 min. Subsequently, the cells were permeablized with 0.2 % (v/v) Triton X-100. After 1 hour incubation with appropriate primary antibodies diluted at 1:200 in PBS containing 5 % (v/v) goat serum and 5 % (v/v) bovine serum albumin at room temperature, the cells were washed three times with PBS. The cells were then incubated with flourescein isothiocyanate conjugated secondary antibodies diluted at 1:200 in PBS with 5% (v/v) goat serum and 5% (v/v) bovine serum albumin at 4°C for 1 hr and washed three times with PBS. Coverslips were mounted with fluorescence mounting medium reagent (DAKO).

Visualization was done using Olympus IX70 Inverted Microscope (Olympus) or Radiance 2000 Confocal Microscope (BIORAD). Dual labeled cells were viewed for co-localization by superimposing the fluorescent images. The region of overlap in the merged image was displayed as yellow.

CHAPTER 3: RESULTS

In animal and early human isolates, the subgenomic mRNA8 of SARS-CoV was predicted to contain a single ORF 8 (Guan *et.al.,* 2003). The deletion of 29 nucleotides (between T_{27867} and A_{27868} for strain SG2774 (accession No: AY283798) gave rise to two separate ORFs (ORF 8a and 8b) in most human isolates collected at the late stages of the SARS outbreak (Fig.16.).

ORF 8a and 8b are predicted to encode two small proteins, 8a and 8b, and ORF 8 codes for a single protein 8ab, a fusion form of the proteins 8a and 8b. ORF 8a is predicted to encode a 39-amino acid protein; ORF 8b encodes an 84-amino acid protein and ORF 8ab codes for a 122-amino acid protein. This project was concentrated on studying the protein expression, characteristics and functions of proteins encoded by ORF 8a/b, ORF 8a, ORF 8b and ORF 8.

3.1. Cloning and expression of SARS-CoV mRNA 8

Four different fragments were PCR amplified and cloned into pKT0 plasmid in which a Flag epitope was fused to each fragment at its 5' ends. These plasmids are known as pF-8a/b, pF-8a, pF-8b and pF-8ab. Another p8a/b using pKT0 as vector was constructed, in which fragment 8a/b was cloned with its TRS at the 5' end. Diagram of the constructs were shown in Fig.3.1.

Constructs pF8a, pF-8b and pF-8ab were expressed using TnT transcription coupled translation wheat germ extracts (WG) in the presence of [^{35}S] methionine. Single protein bands of 5.3, 10.2 and 14.4 kDa, corresponding to Flag-tagged proteins 8a, 8b and 8ab respectively, were detected (Fig. 3.2a, lanes 3-5).

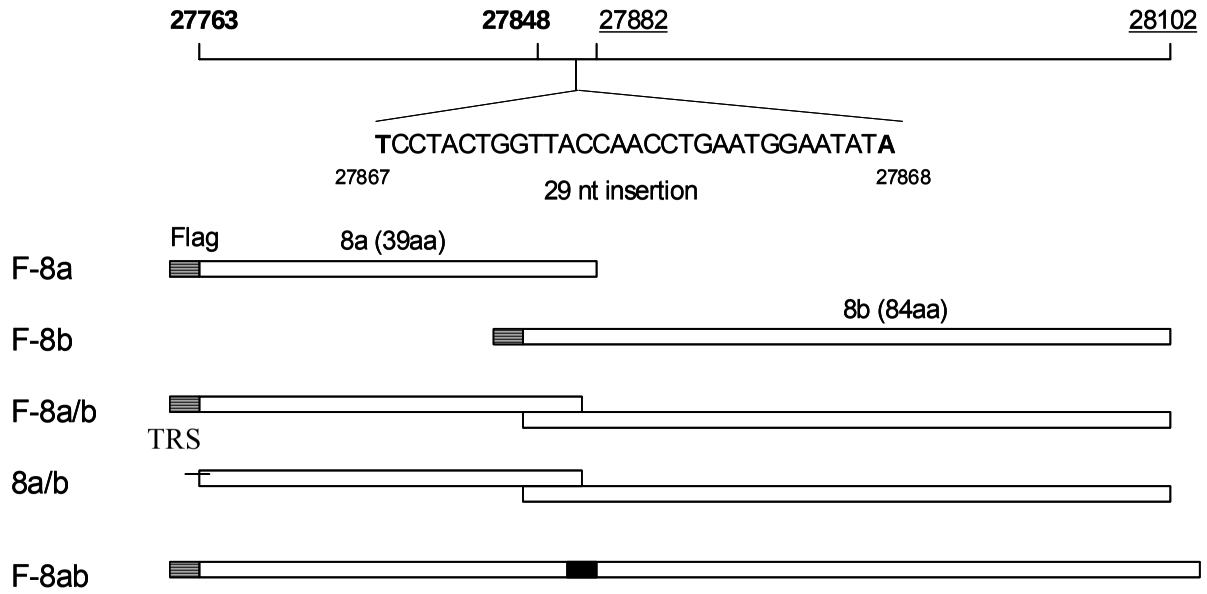

Figure 3.1. Diagram of constructs used in this study
The ORF 8a/b cDNA fragment was amplified by PCR from residue 27763 to 28102 and cloned into pFlag, named pF-8a/b. ORF 8a and ORF 8b cDNA fragments were amplicated individually by PCR and inserted into pFlag, named pF-8a and pF-8b. ORF8ab cDNA fragments was created by using overlapping PCR to insert 29 nucleotides (CCTACTGGTTACCAACCTGAATGGAATAT) into the ORF 8a/b cDNA fragment from residue 27867, and subsequently the fragment was cloned into pFlag, named pF-8ab. In pFlag, ORF sequences were fused with the Flag epitope at their 5' terminal region. The Flag peptide was illustrated by stripped boxes and 29-nucleotide of pF-8ab was illustrated by black box. In p8a/b, ORF 8a/b was cloned with its TRS.

However, in the expression of p8a/b and pF-8a/b (Fig.3.2a, lanes 1 and 2), single bands of sizes 4.3 and 5.3 kDa were detected, corresponding to the unflagged 8a protein only and Flag-tagged 8a, respectively. No protein 8b band was detected.

Expression of the four constructs p8a/b, pF-8a/b, pF-8b and pF-8ab in rabbit reticulocyte lysates (RRL) in the presence of [^{35}S] methionine showed similar results (Fig.3.2b, lanes 1-4). Multiple bands with every increase of approximately 10 kDa were detected in the expression of pF-8b and pF-8ab (Fig.3.2b, lanes 3 and 4). Immunoprecipitation using rabbit anti-8b polyclonal antibodies was carried out in order to investigate whether these bands were related to the 8b region. As shown in Fig.3.2b, the 10.2-kDa 8b and the 14.4-kDa 8ab together with their corresponding ladder bands were precipitated with anti-8b antibodies (lanes 7 and 8). Various ubiquitinated proteins were initially discovered in conjugation with ubiquitin by formation of the typical ladder bands when the proteins were translated in vitro by rabbit reticulocyte lysates (Merrick, 1983; Iwamuro *et.al.,* 1999). Therefore, the patterns of these bands suggested ubiquitination of the proteins 8b and 8ab in the expression system.

Expression of these constructs was then carried out in Cos-7 cells using the vaccinia/T7 expression system. As shown in Fig.3.3a, the expression of Flag-tagged 8a, 8b, and 8ab were detected in cells transfected with the corresponding constructs by Western blot analysis using anti-Flag antibodies (lanes 2-4). Cells were also transfected with p8a/b as a negative control. The absence of protein bands demonstrated the binding specificity of the anti-Flag antibodies (lane 1). Similar multiple bands as observed with *in*

Figure 3.2. Expression of plasmids p8a/b, pF-8a/b, pF-8a, p-F8b and pF-8ab in vitro translation systems.

a. Plasmids p8a/b, pF-8a/b, pF-8a, p-F8b and pF-8ab were *in vitro* translated using wheat germ extracts in the presence of ^{35}S methionine. The proteins were separated in 20% SDS-PAGE and visualized by autography (lanes 1-5). Plasmid p8a/b expressed a 4.3 kDa protein band (lane 1) pF-8a/b (lane 2) and pF-8a (lane 3) expressed a 5.3 kDa protein band. pF-8b (lane 4) and pF-8ab (lane 5) expressed a 10.2 kDa and a 14.4kDa band, respectively.

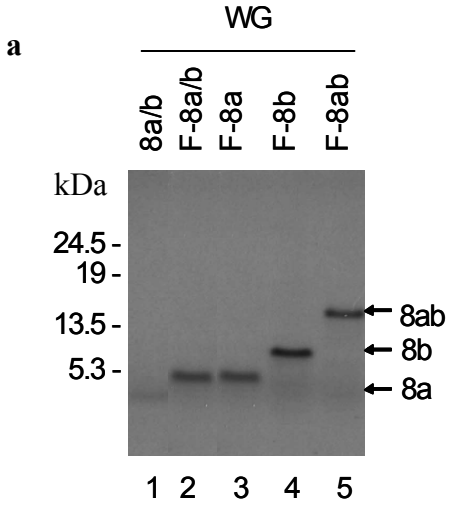

b. Plasmids p8a/b, pF-8a/b, pF-8b and pF8ab were *in vitro* translated using rabbit reticulocyte lysates (RRL) in the presence of ^{35}S methionine (lanes 1 to 4). Subsequently, translation products were subjected to immunoprecipitation (IP) using anti-8b antibodies (lanes 5 to 8). The expression of protein 8b was not observed from p8a/b and pF-8a/b (lanes 1, 2, 5 and 6). The slowly migrating bands were consistently observed in *in vitro* translation products (lanes 3 and 4) and in IP results (lanes 7 and 8) using anti-8b antibody, indicating that protein 8b and 8ab might be ubiquitinated. IP: Immunoprecipitatation.

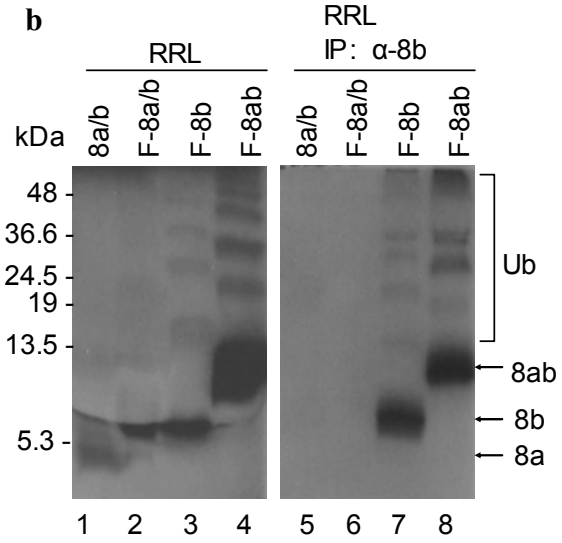

Figure 3.3. Expression p8a/b, pF-8a/b, p-F8b and pF-8ab in Cos-7 cells

a. Plasmids p8a/b, pF-8a/b, p-F8b and pF-8ab were transfected into Cos-7 cells at 4 hour posttransfection with recombinant vaccinia/T7. The proteins were separated by 20% SDS-PAGE and analyzed by Western blot using anti-Flag antibodies. The expression of pF-8a/b was also obtained 5.3 kDa band (lanes 2). The expression of pF-8b and pF-8ab were also detected as bands of 10 and 14.4 kDa, repectively (lanes 3 and 4). The protein expression of p8a/b was not detected due to the specific - binding of anti-Flag antibodies. The typical ladder-bands were detected in the expression of pF-8b (lanen 3) and pF-8ab (lane 4). An extra protein band (8ab*) was observed from expression of pF-8ab, indicating that this protein might have undergone post-translational modification. IB: immunoblotting.

a

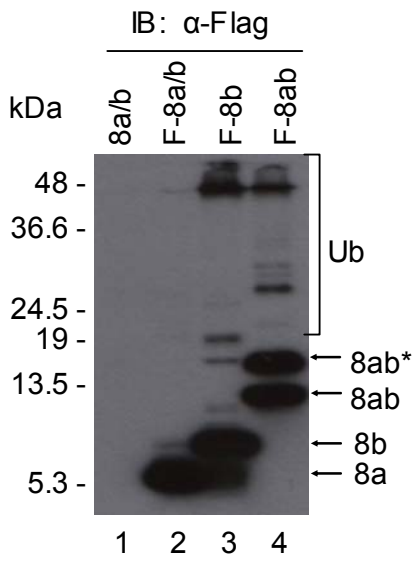

b

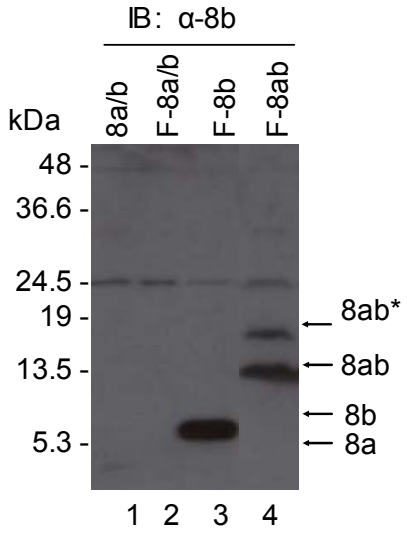

b. Western blot was probed with anti-8b antibodies. The expression of protein 8b from p8a/b and pF-8a/b was not detected.
An extra protein band (8ab*) was observed from the expression of pF-8ab.

vitro translation in RRL were also detected in cells expressing pF-8b and pF-8ab (Fig. 3.3a, lanes 3 and 4).

In a separate analysis using anti-8b antibodies, the 8b protein was only detected in cells transfected with pF-8b and pF-8ab but not in cells transfected with either p8a/b or pF-8a/b (Fig.3.3b). In addition to the 14.4 kDa band, a concomitant band (8ab*) was also observed in cells expressing pF-8ab (Fig. 3.3b, lane 4). It may represent a post-translationally modified 8ab protein.

3.2. Glycosylation of the 8ab fusion protein

Analysis of the protein sequence of 8b and 8ab using the glycomod program predicted a potential N-linked glycosylation site on asparagine residue 43 (N43) of protein 8b and asparagine residue 81(N81) of fusion protein, 8ab.

Based on the above prediction, total cell lysates prepared from cells expressing the Flag-tagged 8b and 8ab proteins were treated with an endoglycosidase, PNGase F to test the possibility of N-linked glycosylation of these proteins. As shown in Fig. 3.4a, the 8ab* band was abolished after the treatment (lane 4), implying that protein 8ab* is the glycosylated form of protein 8ab. On the other hand, the treatment rendered no effect on 8b migration, suggesting that the 8b protein is not modified by N-linked glycosylation (Fig. 3.3a, lane 3).

pF8abM was constructed to introduce a point mutation in the ORF 8ab. The resultant aspartic acid substitution of the N81 residue abolished the glycosylated protein 8ab* band (Fig. 3.5b, lanes 2 and 5) by using both anti-Flag and anti-8b antibodies in Western blot analysis, confirming that N81 is the site for N-linked glycosylation of protein 8ab.

Figure 3.4. The post-translational modification of protein 8ab

a. Cell lysates expressing pF-8b and pF-8ab were treated with PNGase F, an endoglycosidase. Protein expression was anaylized by Western Blot using anti-Flag antibodies.When treated with PNGase F, the upper 8ab* band was disappeared in cell lysates expressing pF-8ab (lane 4), suggesting that it could be N-glycosylated protein 8ab. No effect was observed with the treated protein 8b (lane 3).

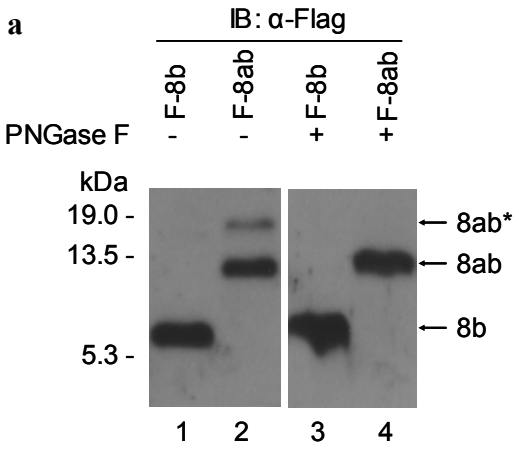

b. Plasmids pF-8ab and pF-8b were expressed in Cos-7 and HeLa cells and analyzed with Western Blot using anti-Flag antibodies. The expression of construct in Cos 7 cells yielded similar amounts of the modified and unmodified 8ab (lane 2), while a higher ratio of the glycosylated form of 8ab protein was detected in Hela cells (lane 4).

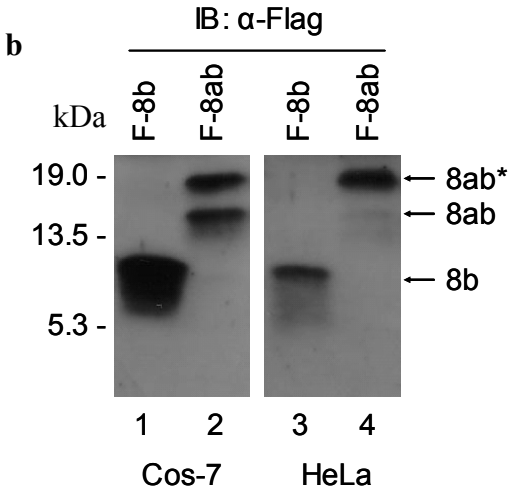

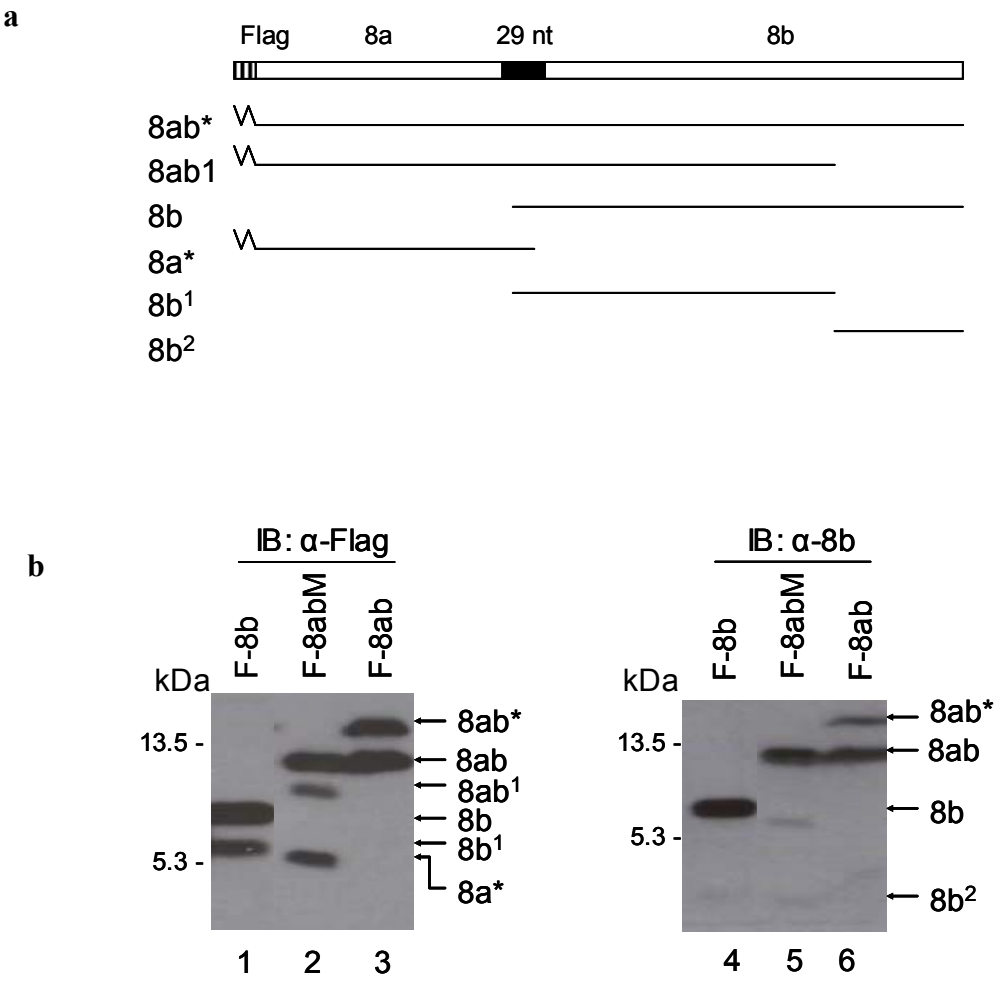

Figure 3.5. The glycosylated site of protein 8ab and the rapid degradation of 8abM in Cos-7 cells.

Three plasmids pF-8b, pF-8abM and pF-8ab were transfected into Cos-7 and analyzed by Western blot with anti-Flag antibody or with anti-8b antibodies.

a. Schematic representation of the cleaved fragments of protein 8b and 8ab*.

b. Disappearance of the upper 8ab* band in expression of pF-8abM in Cos-7 indicated that N81 is the site for N-linked glycosylation of protein 8ab (lanes 2 and 5). In addition to the disappearance of 8ab* band, multiple rapidly migrating bands were observed (lanes 2 and 5). Multiple rapidly migrating bands were also observed in the expression of pF-8b.

Western blot analysis of cells expressing pF8abM using anti-Flag antibody detected two rapidly migrating bands of approximately 10 kDa and 5 kDa (Fig. 3.5b, lane 2). Since Flag sequence was tagged at the N-terminal of protein 8abM, these detected fragments predictably correlate to the N-terminal region of the 8ab (Fig. 3.5a, upper diagram). In addition, analysis using polyclonal anti-8b antibodies which could bind to fragment 8b of protein 8abM detected two other bands of approximately 7 and 3 kDa (Fig. 3.5b, lane 5), correlating to the C-terminal region of the 8abM (Fig. 3.4b, upper diagram). Similar rapidly migrating bands were observed with 8b protein as compared to 8ab* protein bands (Fig.3.5b. lanes 1 and 4).

During the course of this study, it was also noted that F-8ab expression in different cell lines resulted in the detection of variable amounts of the N-linked glycosylated 8ab*. While the expression of construct in Cos 7 cells yielded similar amounts of the modified and unmodified 8ab, a higher ratio of the glycosylated form of the 8ab protein was detected in Hela cells (Fig. 3.4b).

3.3. Ubiquitination of the 8b and 8ab proteins

Rabbit reticulocyte lysates are reported to contain a variety of enzymes and substrates to support various modifications, such as ubiquitination, of translated proteins (Starr *et.al.,* 1990; Sanford *et.al.,* 1991; Tibbles *et.al.,* 1995). The detection of typical ladder bands of the 8b and 8ab proteins when the proteins were expressed in rabbit reticulocyte lysates indicates that they may be ubiquitinated (Fig. 3.2b lanes 3 and 4). Hence, the possibility of ubiquitination of proteins 8b and 8ab was further studied in intact cells.

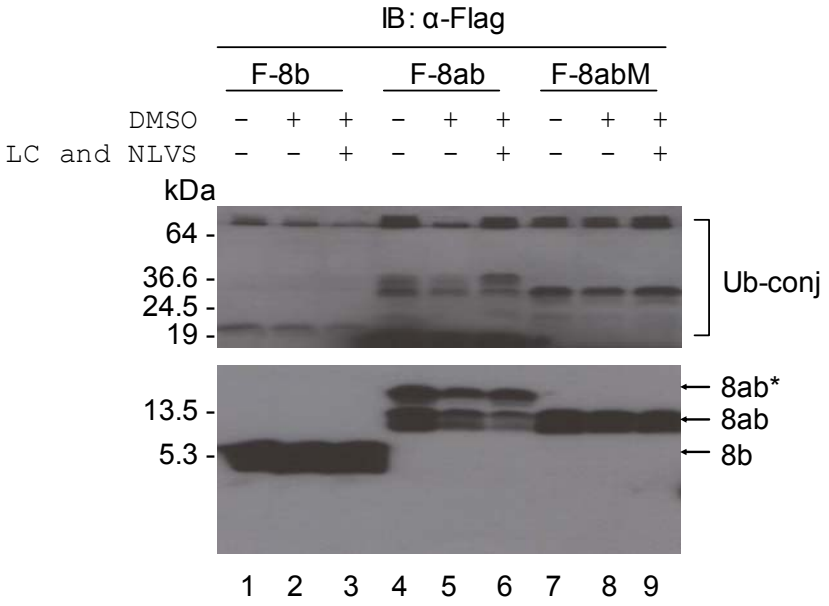

Figure 3.6. Analysis of the ubiquitination of protein 8b, 8ab and 8abM
Plasmids pF-8b, pF-8ab, and pF-8abM were expressed in Cos-7 in the presence or absence of lactacystin (LC) and NLVS. Since DMSO may affect the protein translation, cells was separated into untreatment, DMSO treated and LC and NLVS treated samples. Protein expression was analyzed by Western blot using anti-Flag antibody. The accumulation of larger protein bands but not the full-length 8ab was observed in cells treated with LC and NLVS, indicating that this protein was conjugated with ubiquitin (lanes 4 to 6). This effect was not observed with the larger forms of protein 8b and 8abM.

Proteasome inhibitor lactacystin (4 μM) and NLVS (8 μM) dissolved in DMSO was added to the culture medium 6 hours post-transfection to prevent degradation of the ubiquinated products. As DMSO may affect the translation process, DMSO was separately added as a control. In the presence of DMSO alone, less transfected proteins were expressed (Fig. 3.6, lanes 5 and 6). Addition of lactacystin and NLVS resulted in the specific accumulation of the larger bands in cells over-expressing F8ab, but has no effect on the full length and the glycosylated form (Fig. 3.6, lane 6). This indicated that these bands represented the ubiquitin-conjugated forms of F8-ab. However, this effect was not observed in cells expressing F-8b and F8-abM (Fig. 3.6, lanes 3 and 9).

3.4. Binding of 8b and 8ab proteins to mono- and polyubiquitin

To confirm that the 8a and 8ab proteins are posttranslationally modified by ubiquitination, co-expression of these proteins with a Myc-tagged ubiquitin in Cos-7 cells were carried out, and the expression and interaction of the proteins were determined by Western blot and coimmunoprecipitation assays. As shown in Fig. 3.7a, the expression of mono- and poly-ubiquitin was detected in cells transfected with Myc-tagged ubiquitin plasmid. On the other hand, despite the presence of weak poly-ubiquitin bands, the mono-ubiquitin band was not detected in cells co-expressing the Myc-tagged ubiquitin with either 8b (Fig. 3.7a, lane 1) or 8ab (Fig. 3.7a, lane 2).

Immunoprecipitation of cell lysates prepared from these transfected cells with anti-Flag antibody, followed by Western blot analysis with anti-Myc antibody, led to the detection of strong poly-ubiquitin bands in cells co-expressing the Myc-tagged ubiquitin and the Flag-tagged 8ab (Fig. 3.7a, lane 5). Western blot analysis using anti-Flag

antibody of the same membrane showed the detection of massive free and ubiquitin-conjugated 8ab, demonstrating the efficiency of the immunoprecipitation (Fig. 3.7a, lane 8). However, it was observed that much less protein 8b was immunoprecipitated by the anti-Flag antibody in the same blot, possibly due to a lower transfection efficiency of protein 8b (Fig3.7a, lane 7). This explained the detection of much weaker poly-ubiquitin bands in cells co-expressing the Myc-tagged ubiquitin and the Flag-tagged 8b (Fig. 3.7a, lane 4).

Similarly, Western blot analysis using anti-Flag antibody detected Flag-tagged 8b (Fig. 3.7b, lane 2) and 8ab (Fig. 3.7b, lanes 3 and 4) either expressed alone or co-expressed with the Myc-tagged ubiquitin. The same cell lysates were immunoprecipitated with anti-Myc antibody and subsequently analyzed by Western blot with anti-Flag antibody. In addition to the detection of slowly migrating bands of protein 8ab (Fig.3.7b, lane 7), the Flag-tagged 8b (Fig. 3.7b, lane 6) and 8ab (Fig 3.7b, lane 7) were efficiently detected when they were co-expressed with the Myc-tagged ubiquitin. No detection of the 8ab protein was observed when it was expressed on its own (Fig. 3.7b, lane 8). Western blot analysis using anti-Myc antibody of the same membrane showed the detection of mono- and poly-ubiquitin in cells expressing just the Myc-tagged ubiquitin protein (Fig. 3.7b, lane 9). The mono-ubiquitin band was marginally detected when it was co-expressed with 8b (Fig. 3.7b, lane 10), but was not detected when co-expressed with 8ab (Fig. 3.7b, lane 11).

To rule out the effect of cellular deubiquitin hydrolases activity, the immunoprecipitational experiments were repeated in the presence of deubiquitin inhibitor. Similar results were obtained (Fig. 3.8). The co-immunoprecipitation results shown above

Figure 3.7. Immunoprecipitaion and Western blot analysis of the binding of protein 8b and 8ab to ubiquitin.

a. Plasmids pF-8b or pF-8ab and pMyc-Ub were co-expressed in Cos-7 cells in the presence of recombinant vaccinia/T7. Immunoprecipitation of cell lysates was done using anti-Flag antibody, followed by Western blot analysis using anti-Myc and anti-Flag antibodies. Lanes 1 to 3 show the ubiquitin expression in co-transfected cells. Low expression of ubiquitin was observed in co-transfection (lanes 1 and 2). Proteins 8b and 8ab were immunoprecipitated together with ubiquitin in co-transfected cell lysates but not in single transfection (Lanes 4 to 6). The efficiency of immunoprecipitation of protein 8b and 8ab by anti-Flag antibodies shown in lanes 7 to 9. Much less protein 8b was precipitated down by anti-Flag antibodies (lane 4), possibly due to a lower transfection efficiency of protein 8b (lane 7).

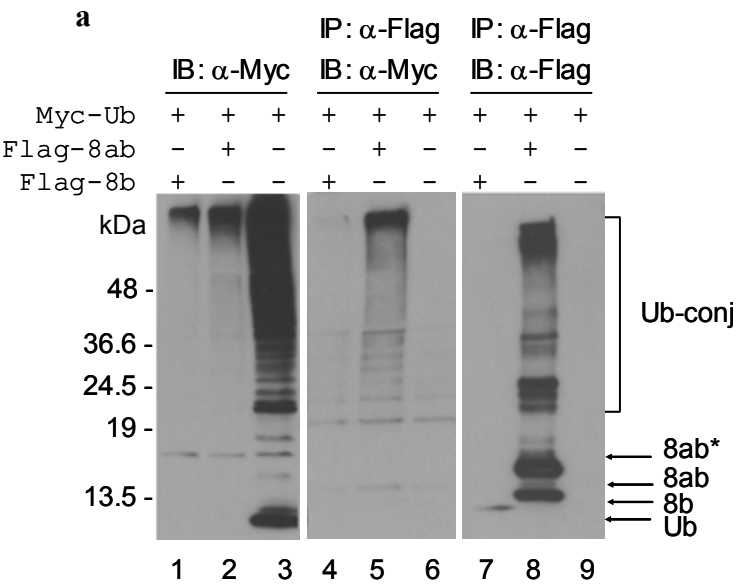

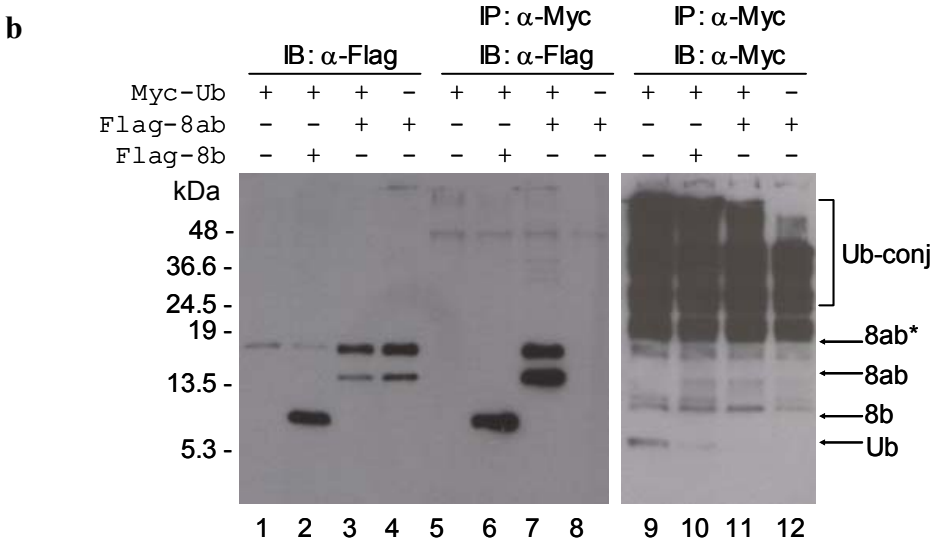

b. The co-transfected cell lysates were immunoprecipitated using anti-Myc antibodies. Lanes 1to 4 show the protein expression of pF-8b and pF-8ab by Western blot analysis using anti-Flag antibodies. Proteins 8b and 8ab were efficiently co-immunoprecipitated by anti-Myc antibodies in the presence of ubiquitin (lanes 6 and 7). Lanes 9 to 12 show the efficiency of immunoprecipitation of ubiquitin using anti-Myc antibodies.

Figure 3.8. Immunoprecipitation with anti-Flag antibody and anti-Myc antibody in the presence of deubiquitin inhibitors

a. Immunoprecipitation of ubiquitin and protein 8b or protein 8ab using -anti-Flag antibodies in the presence of de-ubiquitin inhibitors.Lanes 1 to 4 show the ubiquitin expression in co-transfected cells. Ubiquitin was co-immunoprecipitated with proteins 8b and 8ab in co-transfected cell lysates (lanes 6 and 7) but not in the single transfection (Lanes 5 and 8).

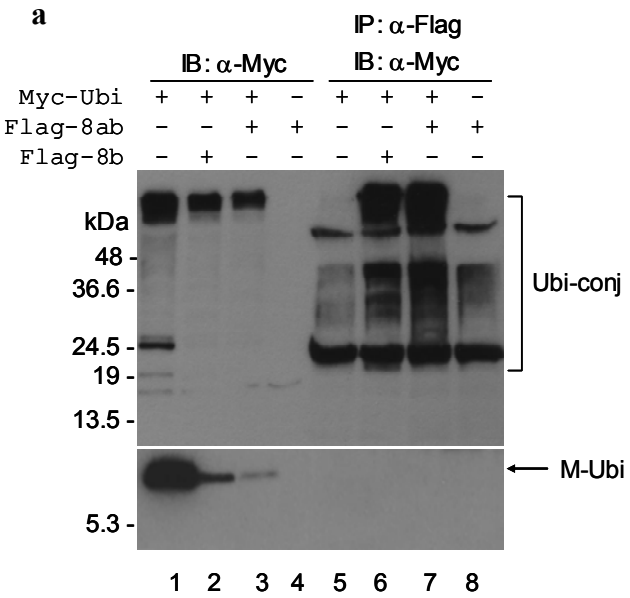

b. Immunoprecipitation of ubiquitin and protein 8b or protein 8ab using anti-Myc antibodies in the presence of deubiquitin inhibitors.
Lanes 1to 4 show the protein expression of pF-8b and pF-8ab by using Western blot with anti-Flag antibodies. Proteins 8b and 8ab were co-immunoprecipitated with anti-Myc antibodies in the presence of ubiquitin and analyzed by Western blot using anti-Flag antibodies (lanes 6 and 7), indicated that proteins 8b and 8ab could bind to ubiquitin non-covalently.

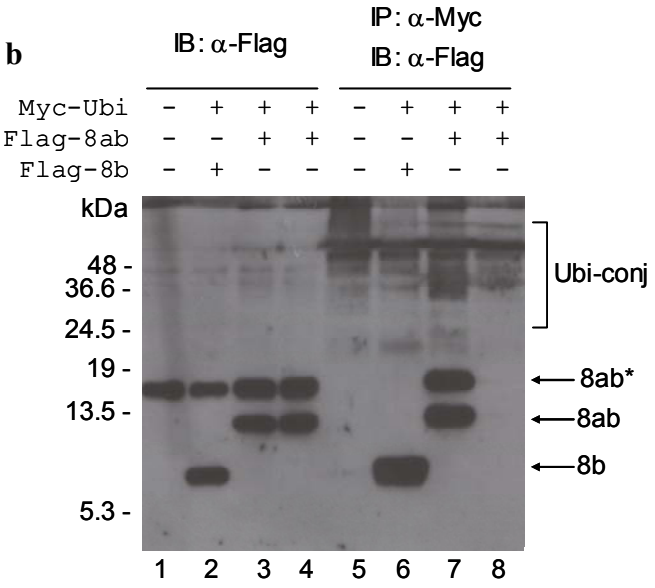

Figure 3.9. Pull down assay of mono- and poly-ubiquitin by GST-8b and GST-8ab proteins

a. Plasmids pGEX-5X-1(GST), pGEX-5X-1/8b (GST-8b) and pGEX-5X-1/8ab (GST-8ab) were expressed in *E.coli* BL21 and proteins were prebound to GST beads.
Equal amounts of GST (lane 1), GST-8b (lane 2) and GST-8ab (lane 3) prebound beads used in pull-down assay were checked by 12% SDS-PAGE and Coommassie blue staining.

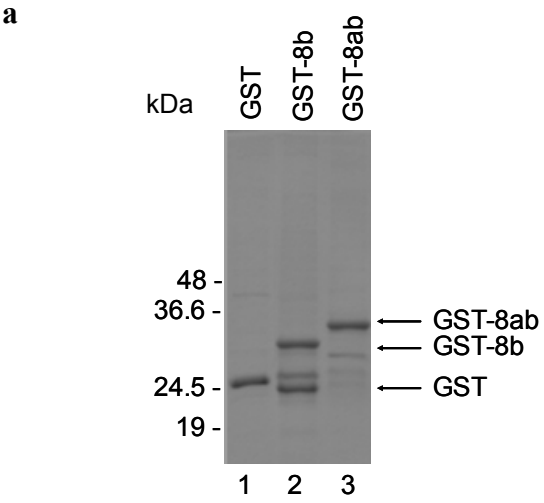

b. Pull-down assay of ubiquitin expressed in cell with or without ^{35}S methionine labelling.
Cell lysates expressing ubiquitin with or without ^{35}S methionie were mixed with protein prebound beads. The beads were separated by 20% SDS-PAGE. The results were analyzed either by autography for the ^{35}S methionie labeled cell lysates or by Western blot using anti-Myc antibodies for unlabeled cell lysates. Mono-ubiquitin and poly-ubiquitin were consistently pull-down with GST-8b and GST-8ab but not with GST (lanes 3, 4, 7 and 8)

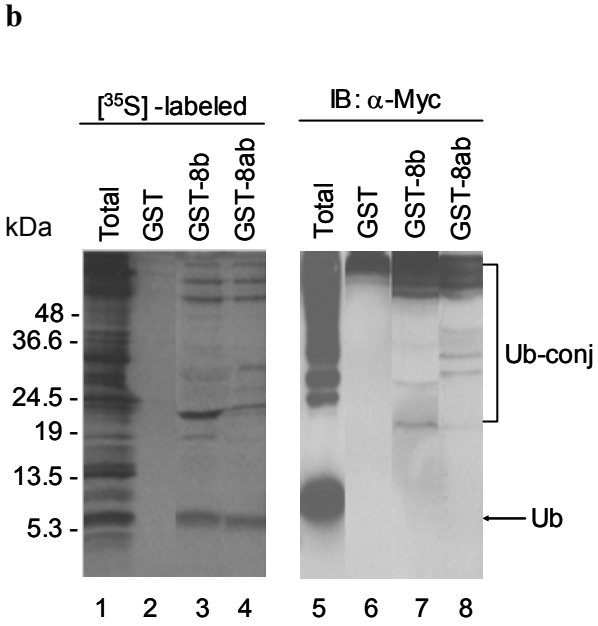

demonstrated that proteins 8b and 8ab could interact with mono- and poly-ubiquitin. To further confirm these results, the 8ab and 8b proteins were expressed in *E. coli* as GST fusion proteins and purified. As shown in Fig. 3.9a, relatively pure GST, GST-8b and GST-8ab proteins were obtained (lanes 1 to 3). Equal amounts of GST, GST-8b and GST-8ab proteins were pre-bound to GST beads prior to a pull-down assay. GST pre-cleared [^{35}S] methionine/cysteine-labeled lysates prepared from cells overexpressing the Myc-tagged ubiquitin were then added to the various pre-bound GST beads and incubated for 2 hours. As shown in Fig. 3.9b, efficient pull-down of mono- and poly-ubiquitin by GST-8b and GST-8ab proteins was observed (lanes 3 and 4). However, no mono- and poly-ubiquitin bands were detected when only GST protein was used (Fig. 3.9b, lane 1). These results confirmed that 8b and 8ab protein can non-covalently bind to the mono- and poly-ubiquitin molecules.

Pull-down experiments were repeated and then analysed by Western blot using anti-Myc antibody. As shown in Fig.3.9b, various forms of poly-ubiquitin were pull-down with GST-8b and GST-8ab but not with GST alone, showing consistent results (lanes 6, 7 and 8). However, a faint band of mono-ubiquitin was observed due to weak binding of ubiquitin to protein 8b and 8ab.

3.5. Binding of 8b and 8ab proteins to ubiquitinated p53 and IκBα.

We next sought to test if the 8b and 8ab proteins can bind to ubiquitinated host proteins. Two proteins, p53 and IκBα, were tested.

First, p53, the Myc-tagged ubiquitin and the Flag-tagged 8b or 8ab were co-expressed in H1299 cells. Immunoprecipitation of the cell lysates were then performed

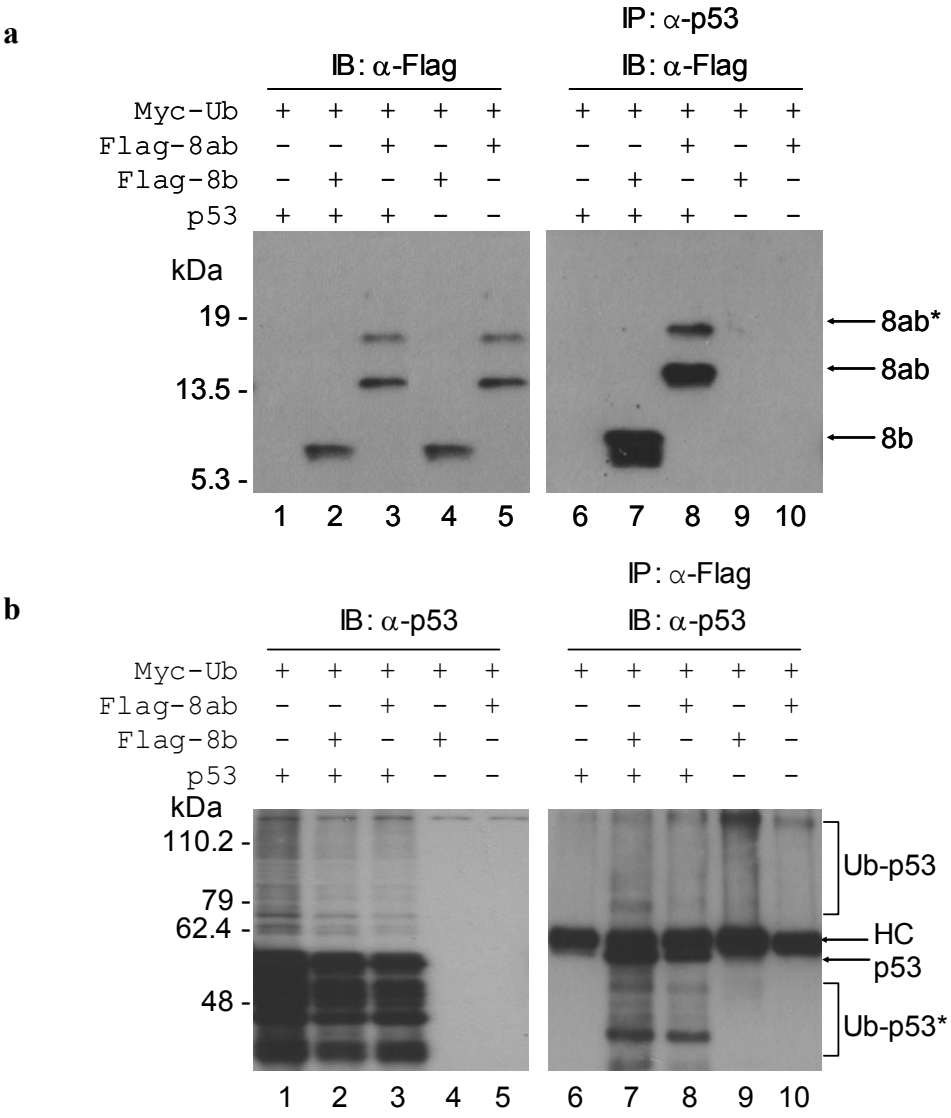

Figure 3.10. Binding of protein 8b and protein 8ab to ubiquitinated p53

p53, the Myc-tagged ubiquitin and the Flag-tagged 8b or 8ab were triple-transfected in H1299 cells.

a. Immunoprecipitation of triple-transfected cell lysates were done with anti-p53 antibodies. Lanes 1 to 5 show western blot results analyzing the expression of protein 8b and 8ab by anti-Flag antibodies. Protein 8b and protein 8ab were found to co-immunoprecipitate with anti-p53 antibodies in the presence of both p53 protein and ubiquitin but not in the presence of ubiquitin alone (Lane 7 and 8).

b. The expression of ubiquitin-conjugated full-length p53 and full-length p53 in triple-transfected cell lysates were analyzed by Western blot using anti-p53 antibodies (Lanes 1 to 3). The immunoprecipitation with the cell lysates were carried out with anti-Flag antibodies and the results were analyzed by Western blot using anti-p53 antibodies. The ubiquitin-conjugated full-length p53 and the degraded intermediate form of p53 were co-immunoprecipitated with protein 8b and protein 8ab in the presence of ubiquitin (lanes 7 and 8), indicating the binding of protein 8b and 8ab to p53 in the presence of ubiquitin.

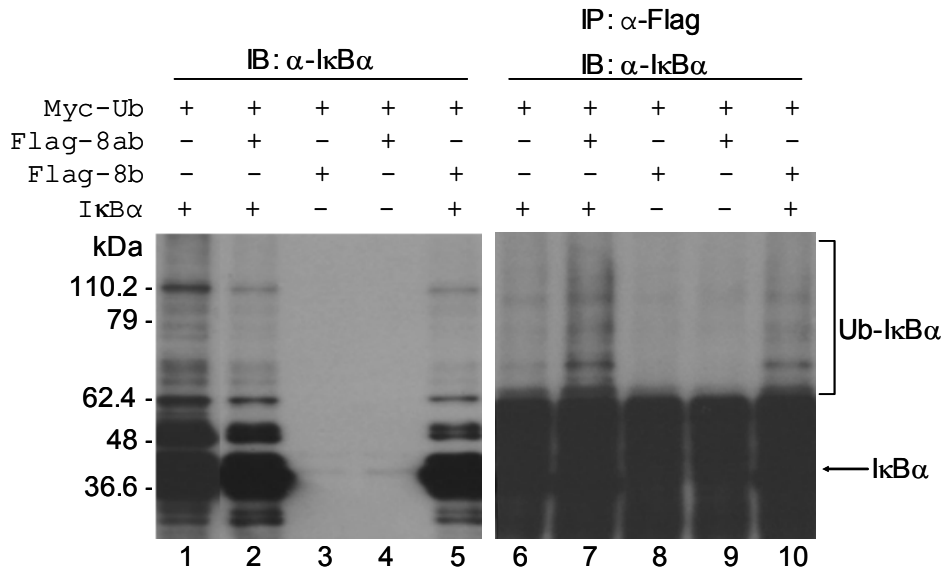

Figure 3.11. Binding of proteins 8b and 8ab to ubiquitinated IκBα
IκBα, the Myc-tagged ubiquitin and the Flag-tagged 8b or 8ab were triple-transfected into Cos-7 cells. The expression of ubiquitin-conjugated IκBα in triple-transfected cell lysates was analyzed by Western blot using anti- IκBα antibodies (Lanes 1 to 3). Immunoprecipitation was done with anti-Flag antibodies and protein expression was analyzed by Western blot using anti- IκBα antibodies. The ubiquitin-conjugated IκBα were also co-immunoprecipitated with proteins 8b and 8ab (lanes 7 and 10).

either with anti-p53 or anti-Flag antibody. As shown in Fig. 3.10a, the 8a and 8ab proteins were efficiently precipitated by an anti-p53 antibody when they were co-expressed in cells with p53 and the Myc–tagged ubiquitin (lanes 7 and 8). The 8b and 8ab protein were not detected in the same co-immunoprecipitation experiments when the two proteins were co-expressed with the Myc–tagged ubiquitin (lanes 9 and 10). Immunoprecipitation of the cell lysates with anti-Flag antibody led to the detection of the ubiquitin-conjugated full-length p53 (Ub-p53) and its putative degraded intermediate forms (Ub-53*) by Western blot with anti-p53 antibody (Fig. 3.10b, lanes 7 and 8). In the same assay, the non-conjugated p53 was also detected (Fig. 3.10b, lanes 7 and 8).

Similarly, co-expression of 8b or 8ab proteins with IκBα and the Myc-tagged ubiquitin led to the detection of the ubiquitinated IκBα (Fig. 3.11, lanes 7 and 10) in the co-immunoprecipitation experiments when anti-Flag antibody and anti-IκBα were used for immunoprecipitation and Western blot, respectively.

3.6. Binding of the 8b and 8ab proteins to Interferon regulatory factor 3 (IRF 3)

SARS-CoV was found to be an inefficient IFN-β inducer because it was reported to affect IRF3, an upsteam stimulator of IFN-β gene (Cheung *et.al.,* 2005). Upon the virus infection, IRF3 can be translocated to the nucleus, and be phosphorylated, homodimerized before binding to its coactivator protein CREB-binding protein (CBP) to stimulate the transcription of IFN-β gene (Hiscott *et.al.,* 1999; Garcia *et.al.,* 2001; Suhara *et.al.,* 2002). Spiegel M. *et.al* (2005) observed that upon infection with SARS-CoV, IRF3 was found to be sequestered in the cytoplasm and it was neither phosphorylated nor homodimerized, and failed to bind to its coactivator protein CBP. Currently no SARS-CoV proteins have

been reported to bind to IRF3. We therefore tested whether the 8a, 8b and 8ab proteins can bind to IRF3. Co-expression of these proteins with IRF3 was carried out in Cos-7 cells. The expression and interaction of these proteins were determined by Western blot and coimmunoprecipitation.

Expression of proteins IRF 3, 8a, 8b and 8ab in cells were shown in Fig.3.12. IRF3 was expressed as a 50 kDa band (Fig.3.12a, lanes 1 to 4). Immunoprecipitation of cell lysates prepared from these transfected cells were performed in the presence of anti-IRF3 antibody, followed by Western blotting with anti-Flag antibody. A strong band of the 8b protein (Fig.3.12b, lane 8) and weak bands of protein 8ab and its glycosylated 8ab protein form were detected (Fig.3.12b, lane9), indicative of a plausible binding between these SARS-CoV proteins with IRF3. No 8a protein band could be observed (Fig.3.12b, lane 6).

Immunoprecipitation using anti-Flag antibody and Western blotting using anti-IRF3 were carried out. The interaction was again observed when the IRF 3 were coimmunoprecipiated in samples where it was co-expressed with either proteins 8b or 8ab, but not with protein 8a (Fig.3.12a, lanes 7, 8 and 9). The coimmunprecipitation of IRF3 with the 8b protein was more efficient than with 8ab protein.

Figure 3.12. Binding of proteins 8b and 8ab to IRF 3

a. Plasmids pF8a, pF8b and pF8ab were coexpressed with IRF 3 in Cos-7 cells. Cell lysates were immunoprecipitated with anti-Flag antibodies and detected with Western blot using anti-IRF3 antibody. The expression of IRF 3 in the cell lysates were analyzed by western blot using anti-IRF 3 antibodies (lanes 1 to 5). IRF 3 was immunoprecipitated with proteins 8b (lane 8) and 8ab (lane 9) but not with protein 8a (lane 2) in the co-expression. Single expression of protein 8ab was used as the control for the immunoprecipitation (lane 10). Increasing amount of IRF 3 was precipitated with protein 8b as compared to protein 8ab.

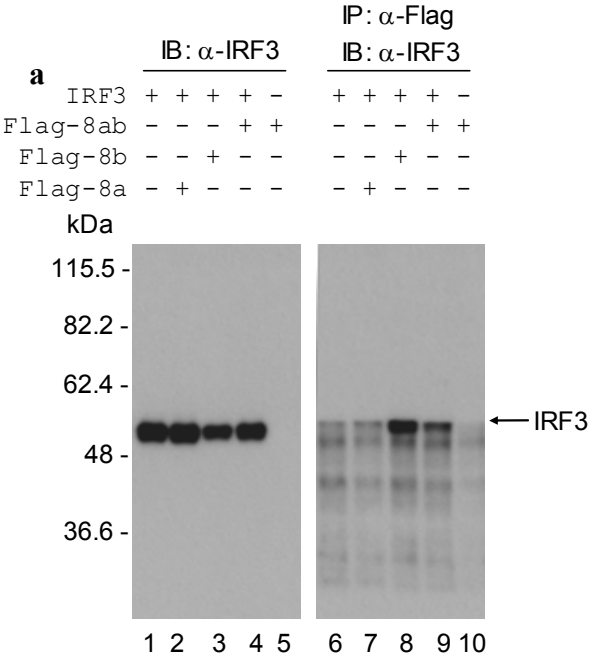

b. The co-transfected cell lysates were immunoprecipitated with anti-Flag antibodies and detected with Wester blot using anti-IRF3 antibody.
The expression of protein 8a, 8b and 8ab were analyzed by western blot using anti-Flag antibodies (lanes 1 to 5).
Consistenly, proteins 8b and 8ab but not protein 8a was immunoprecipitated by anti-IRF 3 antibodies (lanes 8 and 9).

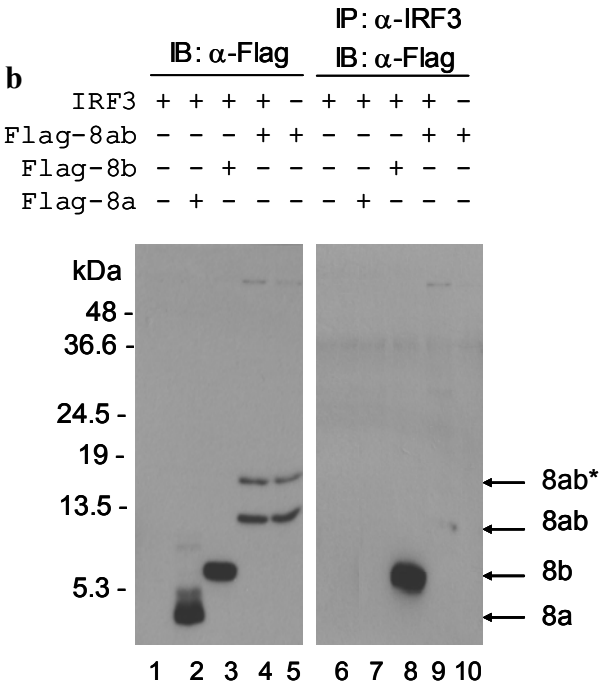

3.7. Subcellular localization of 8a, 8b and 8ab proteins

The Flag-tagged 8a, Flag-tagged 8b and Flag-tagged 8ab cDNA fragments were cloned into pXJ 40 vector in order to express these proteins in Hela cells independently from the recombinant vaccine/T7.

Subcellular localization of the Flag-tagged 8a, 8b and 8ab in HeLa cells were studied by indirect immunofluorescence with anti-Flag antibody and specific markers for various cellular compartments. The nucleus was stained with DAPI, which binds specifically to chromosome DNA (Fig 3.13, panels B, D and H); the Golgi apparatus was stained with p230 (Golgi marker) (Fig.3.14a, panels B, D and H); and the ER was stained with antibody against calnexin - an ER resident protein (Fig.3.14b, panels B, D and H). The results showed that the 8a, 8b and 8ab proteins did not co-localise with the nucleus and was thus found predominantly in the cytoplasm (Fig. 3.13). Co-staining with the Golgi markers was also not detected for any of the three proteins (Fig.3.14a). Immunofluorescent staining of cells expressing the Flag-tagged 8b protein showed that the protein is localized to the perinuclear region with the ER punctated staining pattern (Fig. 3.14b, panels D, E and F). The immunofluorescence signal for 8a and 8ab protein, on the other hand, only partially overlapped with the ER marker (Fig. 3.14b, panels A-C and G-H). Hence the precise localization of the two proteins in the transfected cells is yet to be determined.

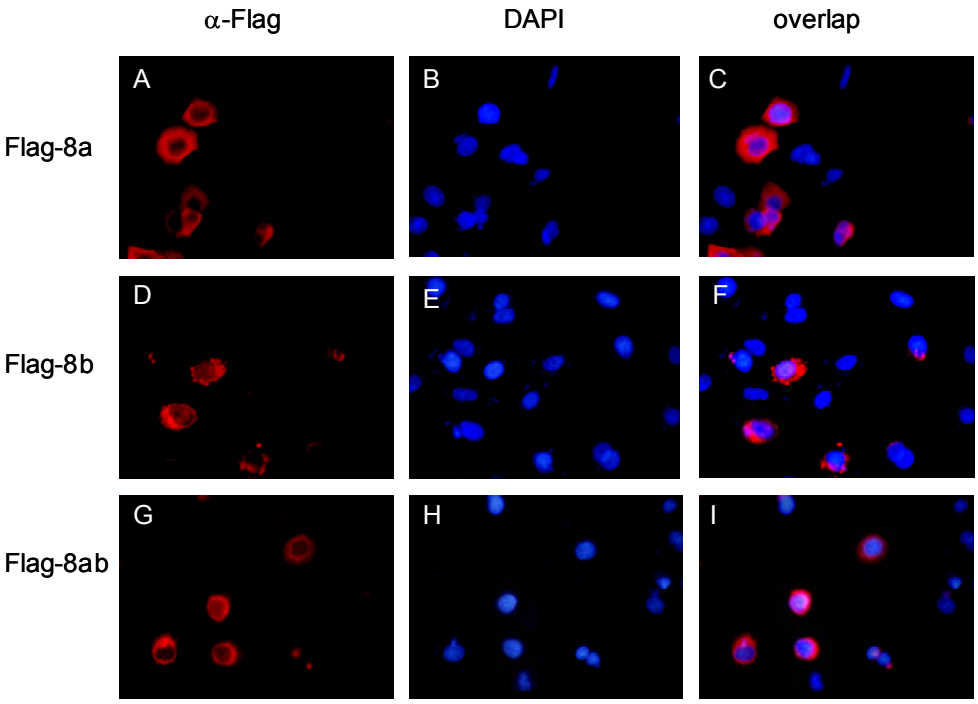

Figure 3. 13. Cytoplasmic localization of proteins 8a, 8b and 8ab
pXJ/F-8a, pXJ/F-8b and pXJ/F-8ab were transfected into HeLa cells. Indirect immunofluorescent staining was carried out at 24 h post-transfection with mouse anti-Flag and followed with anti-mouse secondary antibodies conjugated with flourescein isothiocyanate (panels A, D and G). Nucleus was visualized by staining with DAPI (Panels B, E and H). Panels C, F and I represents the merged images. All images were taken using Olympus IX70 Inverted Microscope (Magnification: 400x)

Figure 3.14. The ER localization of protein 8b

a. Indirect immunofluorescent staining was done using mouse anti-Flag and rabbit anti-p230 antibodies. Theses proteins were detected by anti-mouse and anti-rabbit secondary antibodies conjugated with flourescein isothiocyanate. Panels A, D and G represented the localization of protein 8a, 8b and 8ab in HeLa cells. Golgi apparatus was visualized in panels B, E and H. Panels C, F and I represent the merged images. All images were taken using Radiance 2000 confocal microscope (BIORAD) with magnification 600x. None of the proteins were co-localized with Golgi.

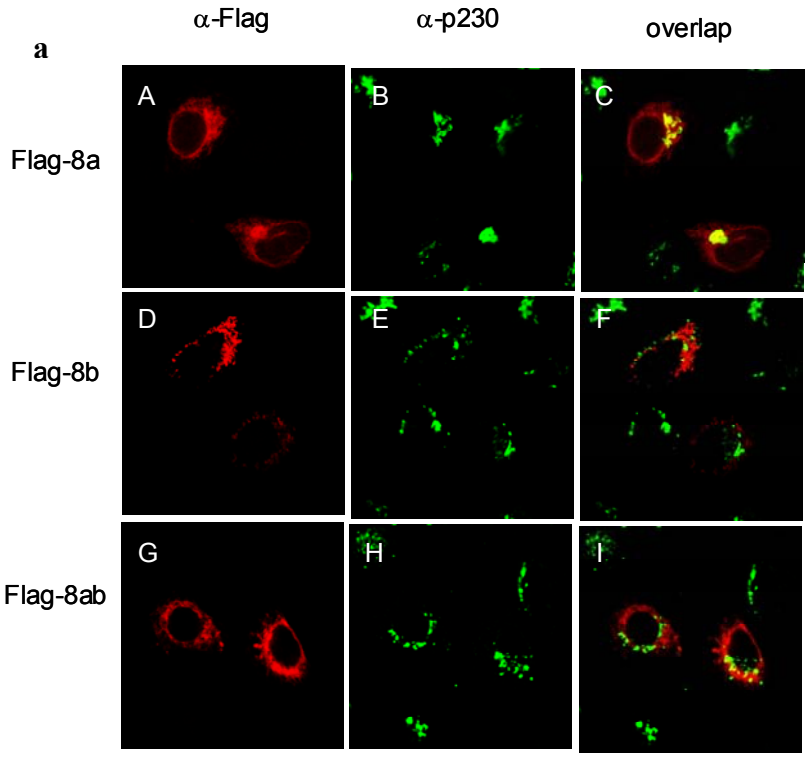

b. The dual staining of HeLa cells was done similarly with ant-Flag antibodies and anti-calnexin, an ER marker. Protein 8b but not protein 8a or protein 8ab was co-localized with ER.

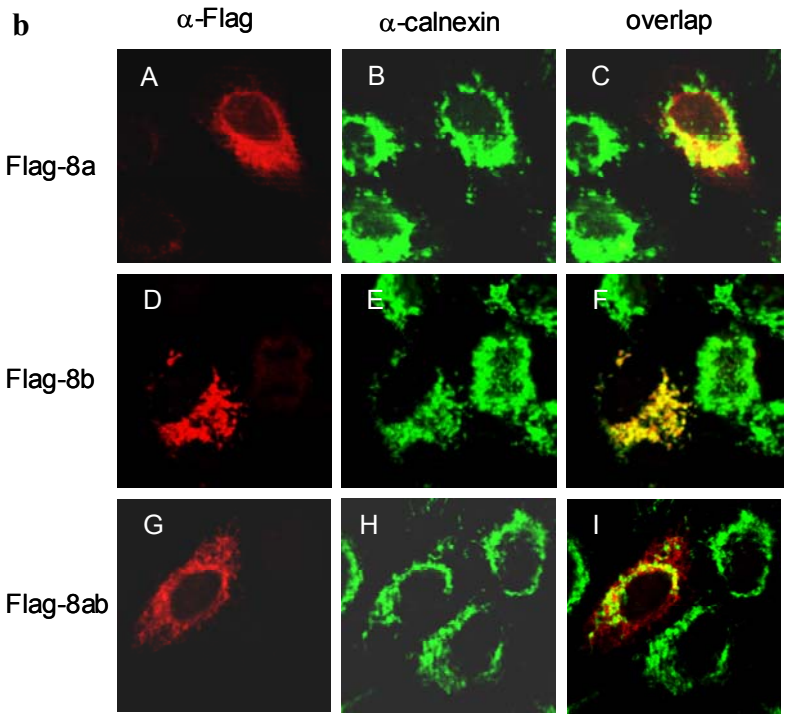

CHAPTER 4: DISCUSSION

4.1. Expression of protein 8a, 8b and 8ab from subgenomic mRNA 8 of SARS-CoV

In this study, ORF 8a was expressed in either wheat germ extracts or rabbit reticulocyte lysates. The expression of the protein was also observed in Cos-7 cells. Similarly, the translation of ORF 8ab was observed in all the translation systems used in this study. In contrast, ORF 8b was only expressed when the ORF was cloned singly, independent of ORF 8a/b.

ORF 8a was expressed as a 5.3 kDa Flag-tagged protein from pF-8a and pF-8a/b (Fig. 3.3a and b). In either wheat germ extracts or rabbit reticulocyte lysates, the expression of p8a/b gave rise to a 4.3 kDa protein band, equivalent to the predicted size of protein 8a. However, due to the lack of a specific antibody, protein 8a from p8a/b could not detected in cells using non-radioactive methods.

In SARS-CoV genomic RNA, putative ORF 8a sits immediately downstream of a strong body TRS (AGUCUAAACGAA**AUG**)(Snijder *et.al.,* 2003). TRSs are known as regulatory sequences for the transcription of negative strand RNAs, which serve as templates for subgenomic mRNA synthesis. In fact, the subgenomic mRNA 8 was documented to be synthesized in SARS-CoV infected cells (Thiel *et.al.,* 2003). The leader sequence and the 5' cap of genomic and subgenomic mRNA could recruit the translation initiation complex including the 40S ribosomal subunit (Tahara *et.al.,* 1994). The ribosome then scans the mRNA and starts translation at the first AUG encountered. Therefore, the 5' most ORF of the genomic and subgenomic mRNA are highly translated. This translation mechanism is known as a cap-dependent mechanism, the so-called ribosomal scanning mechanism (Kozak, 1989). Recently, with the detection of protein 3a

and 7a from the translation of subgenomic mRNA 3 and mRNA 7, respectively, the majority of the 5' most ORF of genomic and subgenomic mRNAs of SARS-CoV are known to express proteins (Yu *et.al.,* 2004, Qui *et.al.,* 2005). In fact, ORF 8a is the 5' most ORF of subgenomic mRNA 8. Hence, ORF 8a is potentially translated by this scanning mechanism. Antibodies against the 8a peptide was present in patients infected with SARS-CoV strains carrying the 29 nucleotide deletion, implying the expression of the protein (Guo *et.al*., 2004; Tan *et.al.,* 2005).

ORF 8ab was expressed from pF-8ab as a 14.4 kDa Flag-tagged protein. Although expression of ORF 8ab from the subgenomic mRNA 8 and the production of antibodies against protein 8ab in patients have not established, protein 8ab was highly likely present. It is because ORF 8ab is the fusion form of ORF 8a and ORF 8b in the subgenomic mRNA 8. Hence, the translation mechanism of ORF 8ab from this subgenomic mRNA 8 must be similar to the translation mechanism of ORF 8a.

By the expression of pF-8b, protein 8b was detected as a 10.2 kDa Flag-tagged protein. However, protein 8b was not translated from the overlapping ORF 8a/b of the constructs p8a/b or pF-8a/b. It was assumed that no detection of the protein was due to the low expression level of ORF 8b as compared with ORF 8a. In order to enrich the ORF 8b product, immunoprecipitation of the *in vitro* translation products labeled with ^{35}S methionine was carried out with anti-8b antibody. However, the protein was still not detected. This ORF was previously speculated to be translated silently for Franfurt-1 and HKU isolates (Snijder *et.al.,* 2003) and no antibodies against 8b peptides are found in SARS-CoV infected patients (Guo *et.al*., 2004).

Although ORF 8b was located downstream of a weak TRS in the subgenomic mRNA 8a/b (CUAAUAAACUC**AUG**) (Marra *et.al.,* 2003), no additional subgenomic mRNA 8b was produced. Thus, if protein 8b is synthesized from ORF8a/b, it would be unlikely translated by the conventional ribosomal scanning mechanism.

There is increasing evidence showing that some coronaviruse proteins are generated by other mechanisms such as leaky scanning or internal ribosome entry. Other coronaviruses uses these mechanisms to translate multi-products from their subgenomic mRNA.

In the leaky scanning mechanism, ribosomes will skip the first AUG and initiate translation at a downstream AUG (Kozak, 1989; Gray and Wrickens, 1998). It has been reported that leaky scanning may operate even when the second initiation site residues as far as 250 nucleotide downsteam of the first (Kozak, 1998). The first AUG of protein 8b is 85 nucleotide residues downsteam of first AUG of protein 8a (Guan *et.al.,* 2003). Thus, protein 8b may translated by leaky scanning.

Also, in internal ribosomal entry mechanism, an RNA fragment at the upstream region of an ORF could form a special RNA structure able to bind ribosomes, resulting in the initiation of translation at a downstream AUG (Gray and Wrickens, 1998; Zuniga *et.al.,* 2004). For example, translation of ORF 3c of the tricistronic subgenomic mRNA 3 of IBV is supported by an internal ribosomal entry site at the upstream RNA fragment of the ORF (Liu *et.al.,* 1992). In the present study, pF-8a/b construct was cloned only with the coding region ORF8a/b; even in p8a/8b construct, the cloned region was extended to the upstream TRS of ORF8a/b. The lack of these important regions in the expression constructs might be a reason for the inability to detect protein 8b from ORF 8a/b.

4.2. Sublocalization of proteins 8a, 8b and 8ab in cells by indirect immunofluorescence

Proteins 8a, 8b and 8ab were not found in nuclei; they are the cytoplasmic proteins. Proteins 8a and 8ab do not reside in the ER or Golgi apparatus. In contrast, protein 8b is an ER protein since its staining image merged with the image of calnexin. The localization of proteins 8a, 8b and 8ab in the cytoplasm supports the hypothesis that these proteins might be involved in the pathogenesis of SARS-CoV.

4.3. Glycosylation of protein 8ab

As predicted by Glycomod Tool Program, protein 8ab potentially binds to glycan at residue N81. A prominent slowly migrating band (8ab*) was detected in cells. This band was designated as N-glycosylated form of the protein by PGNase F treatment and site-directed mutagenesis.

Although predicted with a potential glycosylated sequence motif, the glycosylated form of protein 8b was not detected in Western blot analysis and the protein was not affected by the treatment of PGNase F. In addition, protein 8b was easily degraded. A defective glycosylated protein 8abM was rapidly degraded in cells. The protein was observed with multiple species of intermediate products in the Western blot analysis. Although the two exact cleavage sites on protein 8abM were not defined, they could be narrowed down - one site is on the 8a region and another on the 8b region.

Protein 8ab was not susceptible to cleavage in cells due to its glycosylation. Glycosylation plays a fundamental role in oligomerization, sorting transport and especially in protein folding (Helenius and Aebi, 2001). During glycosylation, glycan

residues are transferred to Asn of the target sequence motif Asn-X- Ser/Thr on a nascent peptidebyoligosaccharyltransferase in eukaryotic cells (Bause, 1983). Then glycan is the "admission ticket" of the protein to go through protein folding or oligomerization, sorting and transport (Helenius and Aebi, 2001).

Change of Asn to Asp of protein 8abM made the protein degraded more easily. In addition, in the absence of 8a region, protein 8b was also easily cleaved although it contains the potential target sequence motif of glycosylation. It is therefore speculated that glycosylation assists the folding of protein 8ab.

The folding process happens in the ER and Golgi apparatus (Ou *et.al.,* 1993; Hammond *et.al.,* 1994). Protein 8ab was not localized in the Golgi apparatus. Hence, protein 8ab might be folded in the ER. Interestingly, calnexin-calreticulin is the cycle involving in the folding process of glycosylated proteins in the ER (Berdard *et.al.,* 1997). In the IF study, protein 8b was co-localized with calnexin and protein 8ab was partially co-localized. This indirect evidence indicates that protein 8b and 8ab might bind to calnexin to get into the folding systems. In the folding process, calnexin and calreticulin bind transiently to glycosylated proteins, and subsequently the calnexin and the calreticulin form a complex with co-chaperon ERp57 (Silvennoinen *et.al.,* 2004). The three-protein complex folds glycosylated proteins by forming correct disulfide bonds (Huppa and Ploegh, 1998). Protein 8ab is rich in cysteine residues at the 8a region. It is likely that protein 8ab acquires its proper conformation from the formation of disulfide bonds in 8a region. In contrast, the folding of protein 8b might be incorrect as it is not able to form disulfide bonds. A properly folded protein 8ab has its cleavage recognition sites masked and therefore it is protected from digestion. Change of Asn to Asp of the

Asn-Val-Thr motif of protein 8abM made the protein lose the glycosylation site. Thus, protein 8abM could not get into the folding systems. Cleavage sites of 8abM protein were exposed and the protein is easily digested.

Glycosylated coronavirus proteins utilize the cellular sorting pathway to complete virion assembly and budding process. S and M proteins of SARS-CoV were highly glycosylated and are sorted to the assembly site by the sorting mechanism in the Golgi apparatus (Huang *et.al.,* 2004; Hofmamnn and Pohlmann, 2004; Nal *et.al.,* 2005). *N*-glycans of S glycosylated protein of SARS-CoV play a role in binding to lectin receptor DC (Yang *et.al.,* 2004) or shielding neutralizing epitopes from antibody recognition (Wei *et.al.,* 2004, Chen *et.al.,* 2005). Using this glycosylation approach to enable proper folding and avoid cleavage could be another means for SARS-CoV in order to protect their proteins.

When pF-8ab was expressed in different cell lines, the amounts of the glycosylated form of 8ab protein were varied. In Cos-7 cells, the amount of unglycosylated protein 8ab was found to be approximately equivalent to the amount of glycosylated 8ab protein, while in HeLa cells, more glycosylated protein was found as compared to unglycosylated protein 8ab. Therefore, human cells seem to support the glycosylation of protein 8ab.

4.4. Ubiquitination of proteins 8b and 8ab

In this study, proteins 8b and 8ab were found to bind non-covalently and covalently to mono and poly-ubiquitin. The ubiquitin interaction was found to facilitate the binding of proteins 8b and 8ab with cellular ubiquitinated proteins, suggesting that proteins 8b and 8ab are involved in the pathogenesis of SARS-CoV.

Proteins 8b and 8ab were initially shown to bind to poly-ubiquitin when the proteins were translated using rabbit reticulocyte lysates. Typical ladder bands of proteins 8b and 8ab were detected. These typical ladder bands were consistently observed in immunoprecipitation using anti-8b antibodies, indicating the ubiquitin conjugation of these proteins. Rabbit reticulocyte lysates is reported to contain varieties of enzymes and substrates to support various modifications of translated proteins including ubiquitination (Starr *et.al.,* 1990; Sanford *et.al.,* 1991; Tibbles *et.al.,* 1995). In addition, various ubiquitinated proteins were initially discovered in conjugation with ubiquitin by formation of typical ladder bands when the proteins were translated in vitro by rabbit reticulocyte lysates (Merrick, 1983; Iwamuro *et.al.,* 1999).

These ladder bands were also observed in the cell. In the presence of proteosome inhibitors, more ladder bands of protein 8ab were accumulated, confirming the ubiquitin conjugation of protein 8ab. The accumulation was not observed with high bands of protein 8b and protein 8abM.

In addition to covalent conjugation with proteins 8b and 8ab, ubiquitin was found to bind non-covalently to these two proteins by co-immunoprecipitation experiments. The non-covalent binding of ubiquitin to proteins 8b and 8ab were further demonstrated by GST- pull down assays.

As they were capable of binding non-covalently and covalently to ubiquitin, proteins 8b and 8ab may contain ubiquitin-binding domains (UBDs). Nine ubiquitin binding domains such as UIM (ubiquitin binding motif), UBA (ubiquitin associated domains) etc. are identified (Hofmann and Falquet, 2001; Shiba *et.al.,* 2004; Slagsvold

et.al, 2005) . Most of UBDs are able to bind to ubiquitin non-covalently and covalently (Hicke *et.al.,* 2005).

Many UBDs were initially discovered by homology search with the identified ubiquitin binding domains (Donaldson, 2003; Hofmann and Falquet, 2003; Hicke *et.al.,* 2005). However, proteins 8b and 8ab do not have any homology with any known UBD, suggesting that they might contain a novel UBDs. Proteins 8b and 8ab but not protein 8a was conjugated with poly-ubiquitin and form complex with mono and poly-ubiquitin. Thus, the novel ubiquitin binding domain of proteins 8b and 8ab is likely located in the 8b region.

The ubiquitin conjugation of UBDs is suggested to assist the formation of a complex between the domain and free mono-poly-ubiquitin. Interestingly, UBDs are able to bind to other ubiquinated proteins (Hicke *et.al.,* 2005), disturbing the function or transportation of polyubiquitinated proteins (Shiba *et.al.,* 2004; Slagsvold *et.al.*, 2005). By immunoprecipitation, proteins 8b and 8ab were established to bind to the ubiquitinated form of p53 and IκBα.

For p53, its ubiquination and degradation by proteosomes play an important role in maintaining a constant level of the protein in cells (Maki *et.al.,* 1996; Prives and Hall, 1999). Binding of 8b and 8ab proteins to polyubiquitinated p53 affects the turnover of the p53 protein in the cell and therefore affects other pathways downstream of p53. Many viral proteins are reported to be involved in inactivation of p53 (Lane and Crawford, 1979; Kao *et.al.,* 1990; Szekely *et.al.,* 1993). For example, E6 oncoprotein of human papillomavirus is reported to inactivate p53 protein by promoting the ubiquitination of p53 protein (Scheffner *et.al.,* 1990).

Various forms of polyubiquitinated IκBα were also detected in co-immunoprecipitation experiments, indicating that proteins 8b and 8ab could possibly bind to the polyubiquitinated forms of IκBα. The ubiquitination and degradation of the IkBα free the cytoplamic nuclear factor kappa β (NFκβ) which then translocated to the nucleus where it can activate transcription of cytokine and chemokine genes. The impairment of the ubiquitination of IkBα affects the activation of NFκβ, leading to the inhibition of the immune systems (Baldwin, 1996).

As p53 and IκBα were chosen randomly, it is suggested the wide effect of proteins 8b and 8ab on ubiquinated proteins.

4.5. Binding of proteins 8b and 8ab to interferon regulatory factor 3

In the immunoprecipitation experiments, IRF 3 was found to bind to proteins 8b and 8ab. Based on the density of immunoprecipitated protein bands, it is noticed that the binding affinity of IRF 3 to protein 8b might be stronger than to protein 8ab.

When host cells are infected, cells quickly produce interferons (IFNs). Newly synthesized IFNs will activate the innate immune systems to resist viruses (Sen, 2001). Most viruses including coronaviruses are known to elicit the interferon pathway, (Aurisicchio *et.al.,* 2000; Levy *et.al.,* 2001; Pei *et.al.,* 2001; Cinatl *et.al.,* 2003). However, in order to increase virus virulence, pathogenic viruses develop various mechanisms to down-regulate the IFN systems by interfering with IFN induction, IFN signaling or the action of IFN-induced effector proteins (Basler *et.al.,* 2002). Obstructing IFN induction is known to be one of the most efficient mechanisms that viruses utilize to counteract the

IFN system. Impairment of the IFN response can cause failure of activation of the innate immune system (Sen, 2001).

Unlike other coronaviruses, SARS-CoV is shown to inhibit the IFN-β producing process. Upon infection of SARS-CoV, no endogenous IFN-β transcripts were produced in infected cells (Cheung *et.al.,* 2005). Interferon regulatory factor 3 is involved in the activation of IFN-β gene (Hiscott *et.al.,* 1999; Iwamura *et.al.,* 2001). Double strand RNA initiates the IFR 3 signaling pathways (Sastre, 2001). After receiving the upstream signal, cytosol IRF 3 is translocated to the nucleus; it is phosphorylated and homodimerizes (Hiscott *et.al.,* 1999). Subsequently, the IRF 3 dimers bind to CBP (Suhara *et.al.,* 2002). This complex can recognize and activate IFN-β with initiation of IFN-β transcription by IRF-3 (Iwamura *et.al.,* 2001). Spiegel M. *et.al* 2005 found that IRF3 is translocated to the nucleus at early stage of SARS-CoV infection but IRF 3 is sequestered in the cytoplasm at late stage of infection; no phosphorylated IRF 3 homodimer is found and hence the impaired IRF3 cannot form complex with CPB. The binding of proteins 8b and 8ab to IRF3 might be the answer for this phenomenon. It is likely that the IRF 3 interaction of proteins 8b and 8ab retain IRF 3 in the cytoplasm, preventing IRF 3 function. However, it is not clear how the binding of proteins 8b and 8ab impairs IRF 3 functioning and whether the binding of these proteins to ubiquitin and IRF 3 leads to the degradation of IRF3. The inactivation of IRF 3 function by protein 8b and 8ab inhibits the IFN response, thus contributing to the virulence of the SARS-CoV.

CHAPTER 5. CONCLUSIONS AND FUTURE DIRECTIONS

5.1. Conclusions

This is the first attempt in trying to gain insights into translation of the subgenomic mRNA 8 of SARS-CoV, ever since the discovery of this virus in 2003. From the study, the following novel findings can be concluded:

1. It was shown that ORFs 8a/b and 8ab expressed proteins 8a and 8ab respectively.
2. Protein 8ab is an N-glycosylated protein. Glycomod Tool Program predicted the N81 residue to the site for glycosylation. The production was verified by PNGase F treatment and site-directed mutagenesis.
3. As the lack of the 8a region, protein 8b is susceptible to rapid degradation.
4. Proteins 8b and 8ab could bind both covalently and non-covalently to mono- and poly-ubiquitin. The ubiquitin-binding domain in these proteins could be novel since no homology to any known ubiquitin-binding domains was found.
5. Ubiquitinated proteins 8b and 8ab interact with the cellular ubiquitinated proteins such as p53 and IκBα. This strongly suggests that ubiquination facilitated the interaction of proteins 8b and 8ab with other ubiquitinated protein.
6. Proteins 8b and 8ab interact with interferon regulatory factor 3. Protein 8b binds more efficiently to IRF 3 than protein 8ab.
7. Proteins 8a and 8ab are localized in the cytoplasm while protein 8b is localized in the ER.

These findings would provide new insights into pathogenesis of SARS-CoV. The hypotheses, herein, lay the ground for other researchers attempting to understand the pathogenesis and signal transduction processes in this important pathogen of human.

First, it is certain that SARS-CoV expresses protein 8a in infected cells. Second, in addition to the utilization of glycan proteins in receptor binding as well as in the assembly process, SARS-CoV also exploits the glycosylation process in infected cells for the folding proteins. Third, cytoplasmic localization of proteins 8b and 8ab and their interaction with IRF 3 may explain the retaining of IRF 3 in the cytoplasm, leading to non-functional IRF 3 upon SARS-CoV infection. Thus, proteins 8b and 8ab may regulate host immunoresponse to SARS-CoV. The more efficient binding of protein 8b to IRF 3 may be attributed to the adaptation of SARS-CoV from animals to human, since most SARS-CoV isolated in the late outbreak stages has ORF 8b instead of ORF 8ab. Finally, the interaction of proteins 8b and 8ab with p53 and IκBα in the presence of ubiquitin indicates the involvement of the proteins in SARS-CoV pathogenesis. In addition, proteins 8b and 8ab might utilize their ubiquitinated forms to bind to cellular ubiquinated proteins and henceforth disrupt the activities of these cellular proteins.

Understanding the signal transduction processes involved in the pathogenesis of SARS-CoV should give us an insight into better vaccine or drug development and hopefully a better control of SARS-CoV.

5.2. Future direction

In this study, the characteristics of these proteins were established in cells expressing individual proteins, but not in the context of virus-infected cells. Protein 8a was found to be expressed in the SARS-CoV infected cells by other groups but the functions of this protein need to be further elucidated. To investigate functions of protein

8a, a yeast two hybrid experiment may be employed to identify cellular interacting proteins.

Protein 8b was not detected from ORF 8a/8b. This could be due to the lack of the elements of subgenomic mRNA 8 during transcription and translation. Therefore, it is necessary to find proper translational systems to clarify expression of ORF 8b. For example, the expression of protein 8b may be studied by using SARS-CoV replicon which contains sufficient transcription elements to produce SARS-CoV subgenomic mRNA.

In this study, protein 8ab was proposed to undergo calnexin-calreticulin cycle. Co-immunoprecipitation experiments may be carried out to study the interaction of protein 8ab with calnexin. Proteins 8b and 8ab are shown to possess ubiquitin-binding domains and may represent a novel group of ubiquitin-binding proteins. As they could bind to p53 and IκBα, it would be interesting to determine the biological consequence of these interactions. Regulation of cellular p53 levels is one of the means many viruses use to increase virulence. The effect of proteins 8b and 8ab on the cellular p53 level may be studied by overexpression of the viral proteins in cells. Also, the significance of the binding of protein 8b and 8ab to ubiquitinated IκBα may be studied by investigating the transcriptional regulation of cytokine and chemokine genes by NFκB. In addition, proteins 8b and 8ab were demonstrated to bind to IRF 3. Further experiments investigating the consequences on nuclear translocation and phosphorylation of IRF 3 in the presence of protein 8b and 8ab may provide further insights into the mechanism of IRF 3 inhibition.

APPENDIX. CONSTRUCTIONS OF PLASMID

pKT0 8a/b: TRS plus ORF 8a/8b fragment from nucleotides 27752 and 28102 was amplified from strain SG2774 (accession No: AY283798) by PCR using TRS-8 forward primer (5' GC**GAATTC**TCTAAACGAACATGAAAC 3') and 8 reverse primer (5' GC**TCTAGA**TTAATTTGTTCGTTTATT 3'). The two primers were incorporated with EcoRI and XbaI endonuclease restriction sites, respectively. The PCR fragment was digested with EcoRI/XbaI and ligated into EcoRI/ XbaI digested pKT0 (Liu *et.al.*, 1994).

pF-8a/b: ORF 8a/8b fragment from nucleotides 27763 and 28102 was amplified from p8a/b by PCR using EcoRV 8 forward primer (5' GG**GATATC**CATGAAACTTCTCAT 3') and 8 reverse primer. The ORF 8a/b fragment was digested with EcoRV and XbaI, then ligated into EcoRV/ XbaI pFlag .

pF-8a: Similarly, 8a fragment was PCR product of pF-8a/b using T7 primer and BamHI 8a reverse primer (5' CGG**GATCC**CTAGTGTTGTACCTTAC 3') and then cloned into EcoRV/XbaI digested pFlag.

pF-8b: Also, the two primers EcoRV 8b forward primer (5' GG**GATATC**CATGTGCTTGAAG-3') and 8 reverse primer were used to amplified fragment from pF-8a/b and then cloned in pFlag..

pF-8ab: This plasmid was cloned by two overlapping PCR. The first round of overlapping PCR was to get 8a plus and 8b plus fragment. The 8a plus fragment was amplified from pFlag 8a using T7 primer (TAATACGACTCACTATAGGG) and downstream 8 deletion primer (5' ATTCAGGTTGGTAACCAGTAGGACAAGGATCTTCAA 3'). Also, the 8b plus fragment was created by using two primers upstream 8 deletion primer (5' TAC

CAACCTGAATGGAATATAAGGTACAACACTAGG 3') and 8 reverse primer. Flag 8ab fragment was obtained in second round of PCR in which the 8a plus and 8b plus were used as templates together with two primers - T7 and 8 reverse primer. The T7 8ab fragment was digested with Bgl II/XhaI and cloned into BamHI/XhaI digested pFlag.

pF-8abM was created by site-direct mutagenesis with a set of commentary primers carrying 2 nucleotide mutation. The two primers were UP primer 5' CATGCACACCTG ATGTTACTATCAA 3' and DOWN primer 5' TTGATAGTAACATCAGGTGTGCAT G 3'.

pXJ/F-8a, pXJ/F-8b and pXJ/F-8ab: pF-8a, pF-8b and pF-8ab were digested with BamHI and XhoI and cloned into pXJ40 digested with Bgl II/ XhoI.

pGEX-5X -1/8b and pGEX-5X-1/8ab: 8b fragment and 8ab fragment was obtained by PCR amplification with two primers-EcoRI forward primer: 5' CCG**GAATTC**CATGTGCTTGAAGATCCTTGTA AGG 3' and 8 reverse primer for 8b fragment and the two primers: EcoRI 8a primer: 5' CCG**GAATTC**CGGATGAAA TTCCTC 3' and 8 reverse primers for 8ab fragment. The two fragments were cleaved with EcoRI and XbaI and then inserted into EcoRI/XbaI digested pGEX-5X-1.

REFERENCES

Arbely E., Z. Khattar, G. Brotons, M. Akkawi, T. Salditt and I. T. Arkin. 2004. A Highly Unusual Palindromic Transmembrane Helical Hairpin Formed by SARS Coronavirus E Protein. J. Mol. Biol. **341**: 769–779.

Aurisicchio L., P. Delmastro, V. Salucci, O. G. Paz, P. Rovere, G. Ciliberto, N. La Monica, and F. Palombo. 2000. Liver-specific alpha 2 interferon gene expression results in protection from induced hepatitis. J. Virol. **74**: 816– 4823.

Baldwin A. S. 1996. The NF-κB and IκB proteins: New discoveries and insights. Annu. Rev. Immunol. **14**:649-681.

Barretto N., D. Jukneliene, K. Ratia, Z. Chen, A. D. Mesecar, and S. C. Baker. 2005. The Papain-Like Protease of Severe Acute Respiratory Syndrome Coronavirus Has Deubiquitinating Activity. J. Virol. **79**:15189-15198.

Bartlam M., H. Yang and Z. Rao. 2005. Structural insights into SARS coronavirus proteins. Curr. Opin. Struct. Biol. **15**: 664–672

Basler C. F., and A. G. Sastre. 2002. Viruses and the type I interferon antiviral system: induction and evasion. Int. Rev. Immunol. **21:**305–337.

Bause E. 1983. Structural requirements of N-glycosylation of proteins. Studies with proline peptides as conformational probes. Biochem. J. **209**: 331-336.

Bedard K., Szabo E., Michalak M., Opas M. 2005. Cellular functions of endoplasmic reticulum chaperones calreticulin, calnexin, and ERp57. Int.Rev. Cytol. **245**: 91-121.

Bosch B. J., R. V. D Zee, C. A. M. Haan, and P. J. M. Rottier. 2003. The Coronavirus Spike Protein Is a Class I Virus Fusion Protein: Structural and Functional Characterization of the Fusion Core Complex. J. Virol. **77**: 8801-8811.

Brierley I., M.E. Boursnell, M. M. Binns, B. Bilimoria, V. C. Blok, T. D. Brown, and S. C. Inglis 1987. An efficient ribosomal frame-shifting signal in the polymerase-encoding region of the coronavirus IBV. EMBO J. **6**:3779-3785.

Brierley I., P. Digard and S. C. Inglis.1989. Characterization of an efficient coronavirus ribosomal frameshifting signal: Requirement for an RNA pseudoknot Cell. **57**: 537-547

Brown, T. D. K., and I. Brierly. 1995. The coronavirus nonstructural proteins, *In* "The Coronaviridae" (*In* S. G. Siddell. Eds.), pp: 191-217. Plenum Press, New York.

Chang R. Y., M. A. Hofmann, P. B. Sethna, and D. A. Brian. 1994. A cis-acting function for the coronavirus leader in defective interfering RNA replication. J. Virol. **68**:8223-8231

Chen Z., L. Zhang, C. Qin, L. Ba, C. R. E. Yi, F. Zhang, Q. Wei, T. He, W. Yu, J. Yu, H. Gao and *et.al.* 2005. Recombinant Modified Vaccinia Virus Ankara Expressing the Spike Glycoprotein of Severe Acute Respiratory Syndrome Coronavirus Induces Protective Neutralizing Antibodies Primarily Targeting the Receptor Binding Region. J. Virol. **79**: 2678-2688

Cheung C. Y., L. L. M. Poon, I. H. Y. Ng, W. Luk, S.F. Sia, M. H. S. Wu, K. H. Chan, K. Y. Yuen, S. Gordon, Y. Guan, and J. S. M. Peiris. 2005. Cytokine Responses in Severe Acute Respiratory Syndrome Coronavirus-Infected Macrophages In Vitro: Possible Relevance toPathogenesis. J. Virol. **79**: 7819-7826.

Cinatl, J., B. Morgenstern, G. Bauer, P. Chandra, H. Rabenau, and H. W. Doerr. 2003. Treatment of SARS with human interferons. Lancet. **362**: 293–294.

Dimitrov D.S. 2004. Virus entry: molecular mechanisms and biomedical applications. Nat. Rev. Microbiol. **2**:109-122.

Donaldson K.M., Li W., Ching K.A., Batalov S., Tsai C.C., Joazeiro C.A. 2003. Ubiquitin-mediated sequestration of normal cellular proteins into polyglutamine aggregates. Proc. Natl. Acad. Sci. U S A. 100: 8892-8897.

Drosten C., S. Gunther, W. Preiser, S. van der Werf, H.R. Brodt, S. Becker, H. Rabenau, M. Panning, L. Kolesnikova, *et.al.* 2003. Identification of a novel coronavirus in patients with severe acute respiratory syndrome. N. Engl. J. Med. **348**: 1967–1976.

Fan K., Wei P., Feng Q., Chen S., Huang C., Ma L., Lai B., Pei J., Liu Y.,Chen J *et. al.* 2004. Biosynthesis, purification, and substrate specificity of severe acute respiratory syndrome coronavirus 3C-like proteinase. J. Biol. Chem. **279**:1637-1642.

Fielding B. C., Y. J. Tan, S. Shuo, T. H. P. Tan, E. E. Ooi, S. G. Lim, W. J. Hong, and P. Y. Goh. 2004. Characterization of a Unique Group-Specific Protein (U122) of the Severe Acute Respiratory Syndrome Coronavirus. J. Virol. **78**: 7311-7318.

Fouchier K. R., M. Schutten, G. Rimmelzwaan, G. V. Amerongen, D. van Riel, J. Laman, T. de Jong, G. van Doornum, W. Lim. 2003a. Newly discovered coronavirus as the primary cause of severe acute respiratory syndrome. Lancet **362**: 263-270.

Fouchier R. A. M., T. Kuiken, M. Schutten, G. V. Amerongen, G. J. J. V. Doornum, B. G. V. D. Hoogen, M. Peiris, W. Lim, K. Stohr and A. D. M. E. Osterhaus. 2003b. Aetiology: Koch's postulates fulfilled for SARS virus. Nature 423, 240.

Goebel S. J., Taylor J., and P. S. Masters. 2004. The 3' cis-acting genomic replication element of the severe acute respiratory syndrome coronavirus can function in the murine coronavirus genome. J. Virol. **78**: 7846-7851.

Gray N. K. and M. Wickens. 1998. Control of Translation Initiation in Animals. Annu. Rev. Cell Dev. Biol. **14**: 399-458.

Guan Y., B. J. Zheng, Y. Q. He, X. L. Liu, Z. X. Zhuang, C. L. Cheung, S. W. Luo, P. H. Li, L. J. Zhang, Y. J. Guan, K. M. Butt, K. L. Wong, K. W. Chan, W. Lim, K. F. Shortridge, K. Y. Yuen, J. S. M. Peiris, and L. L. M. Poon. 2003. Isolation and characterization of viruses related to the SARS coronavirus from animals in southern China. Science. **302**: 276-278.

Guo J. P., M. Petric, W. Campbell and P. L. McGeer. 2004. SARS corona virus peptides recognized by antibodies in the sera of convalescent cases. Virology. **324**:251-256

Hammond C., I. Braakman, A. Helenius. 1994. Role of N-linked oligosaccharide recognition, glucose trimming, and calnexin in glycoprotein folding and quality control. Proc. Natl. Acad. Sci. U S A. **91**: 913-917.

Harcourt B. H., D. Jukneliene, A. Kanjanahaluethai, J. Bechill, K. M. Severson, C. M. Smith, P. A. Rota, and S. C. Baker. 2004. Identification of Severe Acute Respiratory Syndrome Coronavirus Replicase Products and Characterization of Papain-Like Protease Activity J. Virol. **78**:13600-13612.

Helenius A. and M. Aebi. 2001. Intracellular Functions of N-Linked Glycans. Science. **291**: 2364-2369.

Hicke L., H. L. Schubert, C. P. Hill. 2005. Ubiquitin-binding domains. Nat. Rev. Mol. Cell Biol. **6**: 610-621.

Hiscott J., P. Pitha, P. Genin, H. Nguyen, C. Heylbroeck, Y. Mamane, M. Algarte, and R. Lin. 1999. Triggering the interferon response: the role of IRF-3 transcription factor. J. Interferon Cytokine Res. **19**: 1–13.

Ho Y., P.H. Lin, C. Y. Y. Liu, S.P. Lee and Y.C. Chao. 2004. Assembly of human severe acute respiratory syndrome coronavirus-like particles. Biochem. Biophys. Res. Commun. 318: 833-838.

Hofmann H. and S. Pohlmann. 2004a. Cellular entry of the SARS coronavirus. Trends Microbiol.**12**: 466-472.

Hofmann H., K. Hattermann, A. Marzi, T. Gramberg, M. Geier, M. Krumbiegel, S. Kuate, K. Überla, M. Niedrig, and S. Pohlmann. 2004b. S Protein of severe acute respiratory syndrome-associated coronavirus mediates entry into hepatoma cell lines and

is targeted by neutralizing antibodies in infected patients J. Virol. **78**: 6134-6142.

Hofmann H., K. Hattermann, A. Marzi, T. Gramberg, M. Geier, M. Krumbiegel, S. Kuate, K. Uberla, M. Niedrig, and S. Pohlmann. 2004c. S Protein of Severe Acute Respiratory Syndrome-Associated Coronavirus Mediates Entry into Hepatoma Cell Lines and Is Targeted by Neutralizing Antibodies in Infected Patients J. Virol. **78**: 6134-6142.

Hofmann K. and Falquet L 2001. A ubiquitin-interacting motif conserved in components of the proteasomal and lysosomal protein degradation systems. Trends Biochem. Sci. **26**, 347−350.

Hon K. L. E., C. W. Leung, W. T. F. Cheng, P. K. S. Chan, W. C. W. Chu, Y. W. Kwan, A. M. Li, N. C. Fong, P. C. Ng, M. C. Chiu, C. K. Li, J. S. Tam, T. F. Fok. 2003. Clinical presentations and outcome of severe acute respiratory syndrome in children. Lancet. **361**: 1701−1703.

Huang Y., Z. Y. Yang, W. P. Kong, and G. J. Nabel .2004a.Generation of synthetic severe acute respiratory syndrome coronavirus pseudoparticles: Implications for assembly and vaccine production.J. Virol. 2004. **78**: 12557-12565.

Huang, Q., L. Yu, A.M. Petros, A. Gunasekera, , Z. Liu, N. Xu,, , P. Hajduk, , J. Mack, , S.W. Fesik, , E.T. Olejniczak, 2004b. Structure of the N-terminal RNA-binding domain of the SARS CoV nucleocapsid protein. Biochemistry. **43**: 6059–6063.

Huppa J.B., Ploegh H.L. 1998. The eS-sence of -SH in the ER.Cell. **92**:145-148.
Ingallinella P., E. Bianchi, M. Finotto, G. Cantoni, D. M. Eckert, V. M. Supekar, C. Bruckmann, A. Carfi and A. Pessi. 2004. Structural characterization of the fusion-active complex of severe acute respiratory syndrome (SARS) coronavirus. Proc. Natl. Acad. Sci. U.S.A.. **101**: 8709-8714.

Iwamura T., M. Yoneyama, K. Yamaguchi, W. Suhara, W. Mori, K. Shiota, Y. Okabe, H. Namiki, and T. Fujita. 2001. Induction of IRF-3/-7 kinase and NF-kappaB in response to double-stranded RNA and virus infection: common and unique pathways. Genes Cells **6**: 375–388.

Iwamuro S., Saeki M., S. Kato. 1999. Multi-ubiquitination of as nascent membrane protein produced in a rabbit reticulocyte lysates. J. Biochem. **126**: 1999.

Kao C.C., Yew P.R., Berk A.J. 1990. Domains required for *in vitro* association between the cellular p53 and the adenovirus 2 E1B 5KK proteins. *Virology*; **179**: 806–814.

Kozak, M. 1989. The scanning model for translation: an update. J. Mol. Biol. **108**: 229-241.

Ksiazek, T. G., D. Erdman, C. S. Goldsmith, S. R. Zaki, T. Peret, S. Emery, S. Tong, C. Urbani, J. A. Comer, *et.al.* 2003. A novel coronavirus associated with severe acute respiratory syndrome. N. Engl. J. Med. 348 20, pp. 1953–1966.

Kuba K., Y. Imai, S. Rao, H. Gao, F Guo, B. Guan, Y. Huan, P. Yang, Y. Zhang and *et.al.* 2005. A crucial role of angiotensin converting enzyme 2 (ACE2) in SARS coronavirus−induced lung injury. Nat. Med. **11**: 875 - 879.

Lai M. M. C. and Holmes K. V. 2001. Coronaviridae: the viruses and their replication. (in Fields Virology, D. M. Knipe, P. M. Howley, Eds.). pp: 1163-1185. Lippincott Williams & Wilkins, New York.

Lai, M. M. C., and D. Cavanagh. 1997. The molecular biology of coronaviruses. Adv. Virus. Res. 48:1-100.

Lane D.P., Crawford L. 1979. T antigen is bound to a host protein in SV40 transformed cells. Nature; **278**: 261–263.

Lau S. K. P., P. C. Y. Woo, K. S. M. Li, Y. Huang, H. W. Tsoi, B. H. L. Wong, S.S. Y. Wong, S.Y. Leung, K. H. Chan and K. Y. Yuen. 2005. Severe acute respiratory syndrome coronavirus-like virus in Chinese horseshoe bats. Proc. Natl. Acad. Sci. **102**: 14040-14045.

Law P. T. W., C.Wong, T. C. C. Au, C.P. Chuck, S.K. Kong, P. K. S. Chan, K. F. To, A. W. I. Lo, J. Y. W. Chan, Y.K. Suen, H. Y. E. Chan, K. P. Fung, M. M. Y. Waye, J. J. Y. Sung, Y. M. D. Lo, and S. K. W. Tsui. 2005. The 3a protein of severe acute respiratory syndrome-associated coronavirus induces apoptosis in Vero E6 cells J. Gen. Virol. **86**:1921-1930.

Levy D. E., and A. Garcia-Sastre. 2001. The virus battles: IFN induction of the antiviral state and mechanisms of viral evasion. Cytokine Growth Factor Rev. **12**:143–156.

Li F., W. Li, M. Farzan, S. C. Harrison. 2005a. Structure of SARS Coronavirus Spike Receptor-Binding Domain Complexed with Receptor. Science. **309**:1864-1868.

Li F.Q., Xiao H., Tam J.P., Liu D.X. 2005b**.** Sumoylation of the nucleocapsid protein of severe acute respiratory syndrome coronavirus. FEBS Lett. **579** : 2387-2396.

Li Q., L. Wang, C. Dong, Y. Che, L. Jiang, L. Liu, H. Zhao, Y. Liao, Y. Sheng, S. Dong and S. Ma. 2005c. The interaction of the SARS coronavirus non-structural protein 10 with the cellular oxido-reductase system causes an extensive cytopathic effect. J. Clin. Virol. **34**: 133-139.

Li T., Zhang Y., Fu L., Yu C., Li X., Li Y., Zhang X., Rong Z., Wang Y., Ning H., Liang R., Chen W, Babiuk L.A., Chang Z. 2005d. siRNA targeting the leader sequence of SARS-CoV inhibits virus replication. Gene. Ther. **12**:751-761.

Li W., M. J. Moore, N. Vasilieva, J. Sui, S. K. Wong, M. A. Berne, M. Somasundaran, J. L. Sullivan K. Luzuriaga, T. C. Greenough, H. Choe and M. Farzan. 2003. Angiotensin-converting enzyme 2 is a functional receptor for the SARS coronavirus. Nature. **426**: 450-454.

Li, W., Z. Shi, M. Yu, W. Ren, C. Smith, J. H. Epstein, H. Wang, G. Crameri, Z. Hu, H. Zhang, J. Zhang, J. McEachern, H. Field, P. Daszak, B. T. Eaton, S. Zhang, and L. F. Wang. 2005d. Bats Are Natural Reservoirs of SARS-Like Coronaviruses. Science **28**: 676-679.

Liao Q.J., L. B. Ye, K. A. Timani, Y.C. Zeng, Y. L. She, L.Ye and Z. H. Wu. 2005. Activation of NF-κB by the full-length nucleocapsid protein of the SARS Coronavirus. Acta. Biochem. Biophys. Sin. **37**: 607-612

Lipsitch M., T. Cohen, B. Cooper, J. M. Robins, S. Ma, L. James, G. Gopalakrishna, S. K. Chew, C. C. Tan, M. H. Samore, D. Fisman, M. Murray. 2003. Transmission dynamics and control of severe acute respiratory syndrome. Science. **300**: 1966−1970.

Liu D. X. and S. C. Inglis. 1992 Internal entry of ribosomes on a tricistronic mRNA encoded by infectious bronchitis virus. J Virol. **66**: 6143–6154.

Liu D.X., Brierley I., Tibbles K.W., Brown T.D. 1994. A 100-kilodalton polypeptide encoded by open reading frame (ORF) 1b of the coronavirus infectious bronchitis virus is processed by ORF 1a products. J Virol. **68**: 5772-80.

Magiorkinis G., E. Magiorkinis, D. Paraskevis, A. M. Vandamme, M. Van Ranst, V. Moulton, A. Hatzakis. 2004. Phylogenetic analysis of the full-length SARS-CoV sequences: Evidence for phylogenetic discordance in three genomic regions J. Med. Virol. **74**(3):369-372.

Marle V., G., J. C. Dobbe, A. P. Gultyaev, W. Luytjes, W. J. Spaan, and E. J. Snijder. 1999. Arterivirus discontinuous mRNA transcription is guided by base pairing between sense and antisense transcription-regulating sequences. Proc. Natl. Acad. Sci. USA. **96:**12056–12061.

Marra M. A., S. J. Jones, C. R. Astell, R. A. Holt, A. Brooks-Wilson, Y. S. Butterfield, J. Khattra, J. K. Asano, S. A. Barber, S. Y. Chan, A. Cloutier, S. M. Coughlin, *et.al*. 2003. The genome sequence of the SARS-associated coronavirus. Science **300**:1399-1404.

Murray R. S., Cai G. Y., K. J. -Y. Zhang, K. F. Soike and G. F. Cabirac. 1992. Coronavirus infects and causes demyelination in primate central nervous system. Virology. **188**: 274-284.

Nal B., C. Chan, F. Kien, L. Siu, J. Tse, K. Chu, J. Kam, I. Staropoli, B. C. Chaigne, and *et.al*. 2005. Differential maturation and subcellular localization of severe acute

respiratory syndrome coronavirus surface proteins S, M and E J. Gen. Virol. **86**: 1423 - 1434.

Nelson C. A., A. Pekosz, C. A. Lee, M. S. Diamond and D. H. Fremont. 2005. Structure and intracellular targeting of the SARS-Coronavirus Orf7a accessory protein. structure. **13**:75-85.

Ou W.J,. Cameron P.H., Thomas D.Y., Bergeron J.J. 1993. Association of folding intermediates of glycoproteins with calnexin during protein maturation.Nature. **364**:771-776.

Pei J., M. J. Sekellick, P. I. Marcus, I. S. Choi, and E. W. Collisson. 2001. Chicken interferon type I inhibits infectious bronchitis virus replication and associated respiratory illness. J. Interferon Cytokine Res. **21**:1071–1077.

Peiris J. S. M., C. M. Chu, V. C. C. Cheng, K. S. Chan, I. F. N. Hung, L. L. M. Poon, K. I. Law, B. S. F. Tang, T. Y. W. Hon, C. S. Chan, K. H. Chan, J. S. C. Ng, B. J. Zheng, W. L. Ng, R. W. M. Lai, Y. Guan, K. Y. Yuen, and members of the HKU/UCH SARS. 2003. Study Clinical progression and viral load in a community outbreak of coronavirus-associated SARS pneumonia: a prospective study. Lancet. **361**, 1767−1772.

Peiris J., S. Lai, L. Poon, Y. Guan, L. Yam, W. Lim, J. Nicholls, W. Yee, W. Yan, M. Cheung. 2003. Coronavirus as a possible cause of severe acute respiratory syndrome. Lancet, **361**: 1319-1325.

Poon L.L., Guan. Y., Nicholls J.M., Yuen K.Y., Peiris J.S.. 2004. The aetiology, origins, and diagnosis of severe acute respiratory syndrome. Lancet Infect. Dis**. 4**: 663-671.

Prabakaran P., X. Xiao and D. S. Dimitrov. 2004. A model of the ACE2 structure and function as a SARS-CoV receptor. Biochem. Biophys. Res. Commun. **314**:235-241.

Prives C. and A. Hall. 1999. The p53 pathway. Pathol. **187**: 112–126.

Qinfen Z., C. Jinming, H. Xiaojun, Z. Huanying, H. Jicheng, F. Ling, L. Kunpeng, Z. Jingqiang. 2004. The life cycle of SARS coronavirus in Vero E6 cells. J. Med. Virol.**73**: 332-337.

Qiu M., Y. Shi, Z. Guo, Z. Chen, R. He, R. Chen, D. Zhou, E. Dai, X. Wang, B. Si, Y. Song, J. Li, L.Yang and *et.al*. 2005a. Subcellular localization and membrane association of SARS-CoV 3a protein. Virus Res. **109**:191-202.

Qiu M.,Y. Shi, Z. Guo, Z. Chen, R. He, R. Chen, D. Zhou, E. Dai, X.Wang, B. Si,Y. Song *et. al*. 2005b. Antibody responses to individual proteins of SARS coronavirus and their neutralization activities. Microbes Infect. **7**: 882–889.

Raman S. and D. A Brian. 2005. Stem-Loop IV in the 5' Untranslated Region Is a *cis*-Acting Element in Bovine Coronavirus Defective Interfering RNA Replication. J. Virol. **79**: 12434-12446.

Riley S., C. Fraser, C. A. Donnelly, A. C. Ghani, L. J. A. Raddad, A.J. Hedley, G. M. Leung, L. M. Ho, T. H. Lam, T. Q. Thach, P. Chau, K. P. Chan, S. V. Lo, P.Y. Leung, T. Tsang, W. Ho, K. H. Lee, E. M. C. Lau, N. M. Ferguson, R. M. Anderson. 2003. Transmission dynamics of the etiological agent of SARS in Hong Kong: impact of public health interventions. Science. **300**: 1961−1966.

Rota P. A., M. S. Oberste, S. S. Monroe, W. A. Nix, R. Campagnoli, J. P. Icenogle, S. Penaranda, B. Bankamp, K. Maher, M. H. Chen, S. Tong, A. Tamin, L. Lowe, *et.al.* 2003. Characterization of a novel coronavirus associated with severe acute respiratory syndrome. Science **300**:1394-1399.

Rowland R. R., V. Chauhan, Y. Fang, A. Pekosz, M. Kerrigan and M. D. Burton. 2005. Intracellular localization of the severe acute respiratory syndrome coronavirus nucleocapsid protein: absence of nucleolar accumulation during Infection and after expression as a recombinant protein in Vero cells. J. Virol. **79**:1507-11512.

Sanford J., J. Codina, and L. Birnbaumer. 1991. Gamma-subunits of G proteins, but not their alpha- or beta-subunits, are polyisoprenylated. Studies on post-translational modifications using in vitro translation with rabbit reticulocyte lysates**.** J. Biol. Chem. **266**: 9570 - 9579.

Sastre G. A. 2001. Inhibition of interferon-mediated antiviral responses by Influenza A viruses and other negative-strand RNA viruses. Virology. **279:** 375–384.

Sawicki S. G. and D. L. Sawicki. 1990. Coronavirus transcription: subgenomic mouse hepatitis virus replicative intermediates function in RNA synthesis. .J Virol. **64**:1050-1056.

Sawicki S. G. and D. L. Sawicki. 1998. A new model for coronavirus transcription. Adv Exp Med Biol. **440**:215-219.

Schaad M. C. and R. S. Baric. 1994. Genetics of mouse hepatitis virus transcription: evidence that subgenomic negative strands are functional templates. J. Virol. **68**: 8169-8179.

Scheffner M. , Bruce A. Werness , J. M. Huibregtse , A. J. Levine and P. M. Howley. 1990. The E6 oncoprotein encoded by human papillomavirus types 16 and 18 promotes the degradation of p53**. Cell**: 1129-1136.

Sen G. C. 2001. Viruses and interferons. Annu. Rev. Microbiol. **55**:255–281.

Shen S., P. S. Lin, Y. C. Chao, A. Zhang, X. Yang, S. G. Lim, W. J. Hong and Y. J. Tan. 2005. The severe acute respiratory syndrome coronavirus 3a is anovel structural protein . Biochem. Biophys. Res. Commun. **330**:286-292.

Shiba Y., Y. Katoh, T. Shiba, K. Yoshino, H. Takatsu, H. Kobayashi, H.W. Shin, S. Wakatsuki, and K. Nakayama. 2004. GAT (GGA and Tom1) Domain Responsible for Ubiquitin Binding and Ubiquitination J. Biol. Chem. **279**: 7105 - 7111.

Shieh C. K., L. H. Soe, S. Making, M. F. Chang, S. A. Stohlman and M. M. C. Lai. 1987. The 5′-end sequence of the murine coronavirus genome: Implications for multiple fusion sites in leader-primed transcription .Virology. **156**:321-330.

Shwarz B., E. Routledge, S. G. Siddle. 1990. Murine coronavirus nonstructural protein ns2 is not essential for virus replication in transformed cells. J. Vol. **64**: 4784-4791.

Silvennoinen L, J. Myllyharju, M. Ruoppolo, S. Orru, M. Caterino, K.I. Kivirikko, P. Koivunen. 2004. Identification and characterization of structural domains of human ERp57: association with calreticulin requires several domains. J. Biol. Chem. **279**:13607-15.

Simmons G., J. D. Reeves, A. J. Rennekamp, S. M. Amberg, A. J. Piefer, and P. Bates. 2004. Characterization of severe acute respiratory syndrome-associated coronavirus (SARS-CoV) spike glycoprotein-mediated viral entry Proc. Natl. Acad. Sci. **101**: 4240-4245

Slagsvold T., R. Aasland, S. Hirano, K. G. Bache, C. Raiborg, D. Trambaiolo, S. Wakatsuki, and H. Stenmark. 2005. Eap45 in Mammalian ESCRT-II Binds Ubiquitin via a Phosphoinositide-interacting GLUE Domain. J. Biol. Chem. **280**: 19600 - 19606.

Smith A.E. and A. Helenius. 2004. How viruses enter animal cells. Science. **304**: 237-242.

Snijder E. J., P.J. Bredenbeek1, J. C. Dobbe, V. Thiel, J. Ziebuhr, L. L. M. Poon, Y. Guan, M. Rozanov, W. J. M. Spaan and A. E. Gorbalenya. 2003. Unique and conserved features of genome and proteome of SARS-coronavirus, an early split-off from the coronavirus group 2 lineage. J. Mol. Biol. **331**:991-1004.

Spaan W., H. Delius, M. Skinner, J. Armstrong, P. Rottier, S. B. Smeekens, A. van der Zeijst, and S. G. Siddell. 1983. Coronavirus mRNA synthesis involves fusion of non-contiguous sequences. EMBO J. **2:**1839–1844.

Spiegel M., A. Pichlmair, L..Sobrido, J. Cros, A. G.Sastre, O. Haller, and F.Weber. 2005. Inhibition of Beta Interferon Induction by Severe Acute Respiratory Syndrome Coronavirus Suggests a Two-Step Model for Activation of Interferon Regulatory Factor 3. J. Virol. **79**: 2079-2086.

Stadler K., V. Masignani, M. Eickmann, S. Becker, S. Abrignani, H. D.Klenk and R. Rappuoli. 2003. SARS-beginning to understand a new virus. Nat. Rev. Micro. **1**: 209-218.

Starr C.M. and Hanover J.A. 1990. Glycosylation of nuclear pore protein p62. Reticulocyte lysate catalyzes O-linked N-acetylglucosamine addition in vitro J. Biol. Chem. **265**: 6868 - 6873.

Suhara W., M. Yoneyama, I. Kitabayashi, and T. Fujita. 2002. Direct involvement of CREB-binding protein/p300 in sequence-specific DNA binding of virus-activated interferon regulatory factor-3 holocomplex. J. Biol. Chem. **277**: 22304–22313.

Sutton G., E. Fry, L. Carter, S. Sainsbury, T. Walter, J. Nettleship, N. Berrow, R. Owens, R. Gilbert, A. Davidson, S. Siddell, L. L.M. Poon, J. Diprose and *et.al*. 2004. The nsp9 Replicase Protein of SARS-Coronavirus, Structure and Functional Insights. Structure. **12**: 341–353.

Szekely L., Selivanova G., Magnusson K.P., Klein G., Wiman K.G.. 1993. EBNA-5, an Epstein–Barr virus-encoded nuclear antigen, binds to the retinoblastoma and p53 proteins. Proc. Natl. Acad.Sci. USA. **90**: 5455–5459.

Tahara S. M., T. A. Dietlin, C. C. Bergmann, G. W. Nelson, S. Kyuwa, R. P. Anthony and S. A. Stohlman. 1994. Coronavirus Translational Regulation: Leader Affects mRNA Efficiency . Virology, **202**: 621-630

Tan Y. J., P.Y. Goh, B. C. Fielding, S. Shen, C. F. Chou, J. L. Fu, H. N. Leong, Y. S. Leo, E. E. Ooi, *et.al*. 2004a. Profiles of Antibody Responses against Severe Acute Respiratory Syndrome Coronavirus Recombinant Proteins and Their Potential Use as Diagnostic Markers. Clin. Diagn. Lab. Immunol. **11**: 362–371.

Tan Y. J., S. G. Lim, W. J. Hong. 2005b. Characterization of viral proteins encoded by the SARS-coronavirus genome. Antiviral Res. **65**: 69–78

Tan Y. J.,.B. C. Fielding, P.Y. Goh, S. Shen, T. H. P. Tan, S. G. Lim, and W. J. Hong. 2004c. Overexpression of 7a, a Protein Specifically Encoded by the Severe Acute Respiratory Syndrome Coronavirus, Induces Apoptosis via a Caspase-Dependent Pathway. J. Virol. **78**: 14043–1404.

Tan Y., E. Teng, S. Shen, T. H. P. Tan, P.Y.Goh, B. C. Fielding, E.E. Ooi, H. Ch. Tan, S. G. Lim and W. J. Hong. 2004d. A Novel Severe Acute Respiratory Syndrome Coronavirus Protein, U274, Is Transported to the Cell Surface and Undergoes Endocytosis. J. Virol. **78**: 6723-6734.

Tan Y.J., P.Y. Tham, D. Z. L. Chan, C. F. Chou, S. Shen, B. C. Fielding, T. H. P. Tan, S. G. Lim and W.J. Hong. 2005e. The severe acute respiratory syndrome

coronavirus 3a protein up-regulates expression of fibrinogen in lung epithelial cells J. Virol. **79**:10083-10087.

Thiel V., K. A. Ivanov, A. Putics, T. Hertzig, B. Schelle, S. Bayer, B. Weissbrich, E. J. Snijder, H. Rabenau, H. W. Doerr, A. E. Gorbalenya, J. Ziebuhr. 2003. Mechanisms and enzymes involved in SARS coronavirus genome expression. J. Gen. Virol. **84**:2305−2315.

Tibbles K. W., I. Brierley, D. Cavanagh, and T. D. Brown. 1995. A region of the coronavirus infectious bronchitis virus 1a polyprotein encoding the 3C-like protease domain is subject to rapid turnover when expressed in rabbit reticulocyte lysate J. Gen. Virol. **76**: 3059 - 3070.

Tripet B., M. W. Howard, M. Jobling, R. K. Holmes, K. V. Holmes, and R. S. Hodges. 2004. Structural Characterization of the SARS-Coronavirus Spike S Fusion Protein Core. J. Biol. Chem. **279**: 20836 - 20849.

WHO. [online], (cited 15 Oct 2003). Summary of probable SARS cases with onset of illness from 1 November 2002 to 31 July 2003. <http://www.who.int/csr/sars/country/table2003_09_23/en/>.

Wong S. K., W. Li, M.l J. Moore, H. Choe, and M. Farzan. 2004. A 193-Amino Acid Fragment of the SARS Coronavirus S Protein Efficiently Binds Angiotensin-converting Enzyme 2. J. Biol. Chem. **279**: 3197 - 3201.

Xiao X., S. Chakraborti, A. S. Dimitrov, K. Gramatikoff and D. S. Dimitrova. 2003. The SARS-CoV S glycoprotein: expression and functional characterization. Biochem. Biophys. Res. Commun. **312**:1159–1164.

Xu X., Liu Y., Weiss S., Arnold E., Sarafianos S.G., Ding J. 2003. Molecular model of SARS coronavirus polymerase: implications for biochemical functions and drug design. Nucleic Acids Res. **31**:7117-7130.

Yang Z. Y., Y. Huang, L. Ganesh, K. Leung, W. P. Kong, O. Schwartz, K. Subbarao and G. J. Nabel. 2004. pH-Dependent Entry of Severe Acute Respiratory Syndrome Coronavirus is mediated by the Spike Glycoprotein and Enhanced by Dendritic Cell Transfer through DC-SIGN. J. Virol. **78**: 5642-5650.

Yao Y. X., J. Ren, P. Heinen, M. Zambon, and I. M. Jones1. 2004. Cleavage and Serum Reactivity of the Severe Acute Respiratory Syndrome Coronavirus Spike Protein. JID. **190**: 91-98.

Yi C. E., L. Ba, L. Zhang, D. D. Ho, and Z.Chen. 2005. Single Amino Acid Substitutions in the Severe Acute Respiratory Syndrome Coronavirus Spike Glycoprotein Determine Viral Entry and Immunogenicity of a Major Neutralizing Domain J. Virol. **79**: 11638-11646.

You J., B. K. Dove, L. Enjuanes, M. L. DeDiego, E. Alvarez, G. Howell, P. Heinen, M. Zambon, J. A. Hiscox. 2005. Subcellular localization of the severe acute respiratory syndrome coronavirus nucleocapsid protein. J. Gen. Virol. **86**: 3303-3310.

Yu C. J., Y. C. Chenb, C. H. Hsiao, T. C. Kuob, S. C. Change, C. Y. Luf, W. C. Weig, C. H. Leeg, L. M. Huang, M. F. Chang, H. N. Hoa. 2004 Identification of a novel protein 3a from severe acute respiratory syndrome coronavirus. FEBS Lett.. **565**: 111–116.

Yuan X., J. Li, Y. Shan, Z. Yang, Z. Zhao, B. Chen, Z. Yao, B. Dong, S. Wang, J. Chen and Y. Cong. 2005a. Subcellular localization and membrane association of SARS-CoV 3a protein. Virus Res. **109**:191-202.

Yuan X., Y. Shan, Z. Zhao, J. Chen, Y. Cong. 2005b. G0/G1 arrest and apoptosis induced by SARS-CoV 3b protein in transfected cells. Virol J. **17** : 66.

Yuan X., Z. Yao, Y. Shan, B. Chen, Z. Yang, J. Wu, Z. Zhao, J. I. Chen, Y. Cong. 2005c. Nucleolar localization of non-structural protein 3b, a protein specifically encoded by the severe acute respiratory syndrome coronavirus. Virus Res. **114** : 70–79

Zeng R., R. F. Yang, M. D. Shi, M. R. Jiang, Y. H. Xie, H. Q. Ruan, X. S. Jiang, L. Shi, H. Zhou, L. Zhang, X. D. Wu, Y. Lin, Y. Y. Ji, and *et. al*. 2004. Characterization of the 3a Protein of SARS-associated Coronavirus in infected Vero E6 cells and SARS patients. J. Mol. Biol. **341**:271-279.

Zhai Y., F. Sun, X. Li, H. Pang, X. Xu, M. Bartlam, Z. Rao. 2005. Insights into SARS-CoV transcription and replication from the structure of the nsp7–nsp8 hexadecamer. Nat. Struct. Mol. Biol. **12**: 980-986.

Zhang X.W. and Y. L. Yap. 2004. Structural similarity between HIV-1 gp41 and SARS-CoV S2 proteins suggests an analogous membrane fusion mechanism. J. Mol. Struct. **677**:73-76.

Ziebuhr J. 2004. Molecular biology of severe acute respiratory syndrome coronavirus. Curr. Opin. Microbiol. **7**:412-419.

Ziebuhr, J., E. J. Snijder, and A. E. Gorbalenya. 2000. Virus-encoded proteinases and proteolytic processing in the Nidovirales. J. Gen. Virol. **81:**853– 879.

Zuniga S., I. Sola, S. Alonso and L. Enjuanes. 2004. Sequence Motifs Involved in the Regulation of Discontinuous Coronavirus Subgenomic RNA Synthesis J. Virol. **78**:980-994.